”Research Prize Tinnitus & Hearing“ 2025 - Application PD Dr. Patrick Neff, University of Zürich (UZH),

Paper title: “Prediction of acoustic tinnitus suppression using resting-state EEG via explainable AI approach”

This remarkable publication in Scientific Reports (Nature Publishing Group) presents a novel approach to tinnitus research, conducted across University of Zurich and University of Regensburg with 102 participants. The study, designed and executed by the applicant with his engineer PhD candidate, achieves the first successful prediction of acoustic tinnitus suppression from resting-state brain activity, reaching classification accuracies of 98% for sensor/source models and 86% for connectivity models. Independent validation achieved 99.1% accuracy, confirming robustness across different recording systems. The research identifies specific neural biomarkers including gamma and alpha oscillations as strongest predictors of suppression capability, along gamma oscillations with hemispheric specialization patterns, intact intra-auditory networks and selective connectivity patterns, and normalized aperiodic spectral features in suppression-capable individuals. These findings advance understanding of neural mechanisms underlying brief acoustic tinnitus suppression (BATS), provide objective markers for tinnitus subtyping, and a blueprint for a parsimonious approach for explainable AI distinguishing tinnitus cases from controls with any human neuroimaging dataset. The work combines explainable AI techniques with comprehensive EEG analysis, unprecedented in the field regarding scientific rigor and state of the art methodology.

Scientific Innovation This work establishes a new research approach by achieving the first successful prediction of brief acoustic tinnitus suppression using (naive) resting-state neurophysiological data. The application of explainable artificial intelligence with SHAP analysis provides interpretable insights into neural mechanisms, surpassing limitations of traditional ”black box” machine learning approaches by allowing rigid results validation and interpretation of direction of effects. The analytical framework encompasses 744 initial features across spectral power, entropy measures, aperiodic parameters, source-localized activity, and large-scale network connectivity, which are systematically preprocessed and fed into an exhaustive set of fitting classifier algorithms, of which the most stable and best performing one was then chosen to inform the main results. The study reveals novel hemispheric specialization patterns, with alpha power dominance in right hemisphere regions and gamma power predominance in left hemisphere auditory networks. The identification of normalized aperiodic spectral signatures in suppression-capable individuals advances understanding of thalamocortical dynamics in tinnitus as well as predicitive coding in the brain (also elicited by the bi-directional predictive value of gamma in temporal auditory fields). The findings contribute a new, all-encompassing theoretical frameworks for tinnitus pathophysiology and provide mechanistic insights into neural processes underlying acoustic suppression capabilities, which inform both further basic research and clinical applications (e.g. neuromodulation).

Clinical Relevance The research addresses the clinical challenge of tinnitus heterogeneity by providing objective neural biomarkers for subtyping individuals based on their acoustic suppression capability. The 98% prediction accuracy demonstrates potential for identifying individuals with preserved suppression mechanisms, which may inform understanding of tinnitus progression and individual differences. The EEG-based classification approach offers an objective alternative to purely subjective tinnitus assessment methods and satisfies the need for a valid, objective biomarker of the condition. While acoustic suppression represents a trait rather than a treatment, understanding the neural basis of this phenomenon may inform future therapeutic development by identifying preserved neural mechanisms and potential intervention targets. The specific brain regions and frequency bands identified provide candidates for investigating neuromodulation approaches.

Quality of Methodological Implementation The study demonstrates methodological rigor through dual-site validation across University of Regensburg (n=79) and University of Zurich (n=29), with consistent findings replicated across different recording systems and populations. The implementation of 10-fold cross-validation with independent test set evaluation prevents overfitting. Randomized label shuffling controls yielded chance-level accuracy (51.7%), confirming the biological validity of identified patterns. The comparison across ten classifier types demonstrates algorithmic robustness and establishes that findings represent biological rather than computational artifacts - again, unseen or un-conceived in the field to date. The multi-scale analytical approach examines data from sensor-level recordings to source-localized regions to network-level connectivity, providing comprehensive and exhaustive characterization of neural substrates of tinnitus (subtypes).

Interdisciplinarity This research integrates machine learning, neurophysiology, and audiology by applying computational methods to understand neural mechanisms of acoustic tinnitus suppression. The work bridges the general fields of neuroscience, engineering, artificial intelligence and clinical audiology, culminating in a state of the art blueprint of explainable artificial intelligence clinical neuroscience in tinnitus.

Patrick Neff, PD Dr.

Google Scholar

University of Zürich
Scientific group lead, Private Lecturer (Privatdozent)
Interdisciplinary Tinnitus Research Zurich
Department of Otorhinolaryngology, Head and Neck Surgery
Faculty of Medicine
University Hospital and University of Zurich
Frauenklinikstrasse 24
8006 Zürich
Email: patrick.neff@uzh.ch
Phone: +41 44 634 02 39

Swiss Citizen
Private address:
Geissbergstrasse 17
5408 Ennetbaden
Email: patrick.neff42@gmail.com

Education

7.5.2025	Re-habilitation, Department of Otorhinolaryngology, Head and Neck Surgery, Faculty of Medicine, University of Zurich, Supervisor: Prof. Dr. Alexander Huber
26.9.2022	Habilitation, Experimental Psychiatry, Faculty of Medicine, University of Regensburg, Supervisor: Prof. Dr. Rainer Rupprecht
25.8.2017	PhD in Neuropsychology, University of Zürich, Thesis Title: 'Neuroplasticity and -modulation in Tinnitus: Understanding Brain Imprints and Suppression of a Phantom Sound", Supervisor: Prof. Dr. Martin Meyer
9.2012 - 9.2014	MSc in Neuropsychology, University of Zürich, Minors: General Linguistics, Neuroinformatics
9.2008 - 9.2012	BSc in Psychology, University of Zürich, Minors: General Linguistics, Neuroinformatics, Film Studies

Current and past positions

5.2025 - current	Scientific Group Lead and Private Lecturer, Department of Otorhinolaryngology, Head and Neck Surgery, Faculty of Medicine, University of Zurich (fixed position)
10.2022 - 4.2025	Scientific Group and Project Lead, Department of Otorhinolaryngology, Head and Neck Surgery, Faculty of Medicine, University of Zurich
10.2017 - 4.2025	Postdoctoral Research Fellow, Department of Psychiatry and Psychotherapy, Center for Neuromodulation and Multidisciplinary Tinnitus Clinic, University of Regensburg, Germany
10.2021 - 10.2023	Postdoctoral Research Fellow, Medical Image Processing lab (MIPlab), Ecole Polytechnique Federale de Genève (EPFL), Switzerland (SNF Postdoc Return), Supervisor: Prof. Dr. Dimitri Van De Ville
8.2019 - 9.2022	Postdoctoral Research Fellow, Center for Cognitive Neurosciences, University of Salzburg, Austria (SNF Postdoc Mobility), Supervisor: Prof. Dr. Nathan Weisz
10.2018 - 9.2022	Postdoctoral Research Fellow and Vice Group Leader, E-Health Workgroup, University of Regensburg, Germany (SNF Early Postdoc and Postdoc Mobility), Supervisor: Prof. Dr. Winfried Schlee
10.2017 - 1.2021	Postdoctoral Research Fellow and Lecturer, URPP Dynamics of Healthy Aging, University of Zurich, Switzerland
10.2014 - 9.2017	Doctoral Student, Neuroplasticity and Learning in the Healthy Aging Brain, URPP Dynamics of Healthy Aging, Department of Psychology, University of Zürich, Supervisor: Prof. Dr. Martin Meyer
5.2014 - 11.2015	Research Fellow (20%), Institute for Computer Music and Sound Technology, University of the Arts, Zürich, Supervisor: Prof. Dr. Germán Toro-Pérez

Memberships

1.2020 - 4.2025	UNITI (link). Scientific expert
10.2017 - 9.2021	ESIT, H2020 No. 722046 (link). Teaching and supervision
10.2014 - 4.2018	TINNET, EU-Cost Action BM1306 (link). Workgroups Neuroimaging and Database

Review and Editorial Activity

Journal Reviews	BioMed Research International, Brain Stimulation, Brain Topography, Ear and Hearing, European Journal of Neuroscience, F1000 Research, Frontiers Publishing Group, HNO, Human Brain Mapping, International Journal of Audiology, IEEE, Journal of the Association for Research in Otolaryngology, Journal of Neuroscience, Nature Publishing Group, Neuroimage, Neuromodulation, Neuropsychiatric Disease and Treatment, Neurorehabilitation and Neural Repair, Neuroscience Letters, PLOS ONE, Psychophysiology
Editor	Frontiers Publishing Group, J - Multidisciplinary Scientific Journal, Journal of the Association for Research in Otolaryngology
Grant Reviews	American Tinnitus Assocatiation (ATA), Auckland Medical Research Foundation, ESF-FWO, ERC, RNID

Awards and Grants

2018	Research Award, PhD Thesis, Swiss Tinnitus League (STL)
2013	Research Grant, “Fonds zur Förderung des Akademischen Nachwuchses (FAN)”, Züricher Universitätsverein (ZUNIV)

Third Party Funding

2023	Rainwater foundation (USA), ”Objective diagnosis of tinnitus”, 24 months, main applicant (55’000 CHF)
2023	Digitalization Initiative of the Zurich Higher Education Institutions (DIZH), ”SpiN3D: Speech in Noise in a virtual 3D Audio-Environment”, 36 months, co-supervision of 1 PhD student, co-applicant (550’000 CHF), main applicant: Martin Meyer
2023	Züricher Stiftung des Hörens (ZSH) Project, ”Transcranial electrical and acoustic stimulation for tinnitus”, 36 months, main supervision of 1 PhD student, co-applicant (176’000 CHF), main applicant: Nicole Peter
2023	SNF Project, ”Processing Language and Cognition in Chronic Subjective Tinnitus”, 10001F_220304, 48 months, co-supervision of 2 PhD students, co-applicant (605’000 CHF), main applicant: Martin Meyer
2021	SNF Return Grant, ”Auditory phantoms and illusions: towards reproducibility and predictive brain models”, P5R5PS_203068, 12 months, personal career funding, main applicant (108’000 CHF)
2019	SNF Postdoc Mobility, ”Auditory neuroscience in tinnitus: towards better understanding of tinnitus suppression, basic neural mechanisms and treatment effects”, P400PS_186670, 18 months, personal career funding, main applicant (77’000 CHF)
2017	SNF Postdoc Mobility, ”Acoustic stimulation and neuromodulation in tinnitus: towards combined and mobile interventions”, P2ZHP1_174967, 18 months, personal career funding, main applicant (77’000 CHF)

September 30, 2025

Publikationsliste PD Dr. Patrick Neff

1. Originalarbeiten

1. Peter, N., Serventi, J., **Neff, P**., Ettlin, D., Wojczyńska, A.Z., Kleinjung, T., Lukic, N. (2025). Tinnitus in patients with orofacial complaints. Head & Face Medicine 21 (1), 1-13.
2. Shabestari, P.S., Edvall, N.K., Vinding, M.C., Vanneste, S., Lundqvist, D**., Neff, P.,** et al. (2025). Inhibition of Cortical Evoked Responses to Sound Pulses by Preceding Silent Gaps. Journal of the Association for Research in Otolaryngology, 1-15.
3. Cai, D., Groves, E., Défayes, L., Naas, A., Gninenko, N., Shabestari, P.S., et al. (2025). Designing Feedback Stimuli in Neurofeedback: Preliminary Requirements from Experts and Users. 2025 IEEE 38th International Symposium on Computer-Based Medical Systems.
4. Shabestari, P.S., Ribes, D., Défayes, L., Cai, D., Groves, E., Behjat, H.H., et al. (2025). Advances on Real Time M/EEG Neural Feature Extraction. 2025 IEEE 38th International Symposium on Computer-Based Medical Systems.
5. **Neff, P**., Cai, D., Groves, E., Défayes, L., Baez-Lugo, S., Naas, A., Shabestari, P.S., et al. (2025). ANT-Advancing Neurofeedback (in Tinnitus). 2025 IEEE 38th International Symposium on Computer-Based Medical Systems.
6. Kader, H., Marcrum, S.C., Engelke, M., Edvall, N.K., Langguth, B., Mazurek, B., et al. (2025). Classifying Residual Inhibition in the Context of Tinnitus: An Interpretable Machine Learning Approach. 2025 IEEE 38th International Symposium on Computer-Based Medical Systems.
7. Naas, A., Sonderegger, A., Lemay, D.R., Shabestari, P.S., Meyer, M., **Neff, P**. (2025). Auditory Phantom Perceptions (Tinnitus) and Neurofeedback Training 'In the Wild': A Feasibility Study on Home Treatment. 2025 IEEE 38th International Symposium on Computer-Based Medical Systems.
8. Shabestari, P.S., Schoisswohl, S., Wellauer, Z., Naas, A., Kleinjung, T., **Neff, P**. (2025). Prediction of acoustic tinnitus suppression using resting-state EEG via explainable AI approach. Scientific Reports 15 (1), 10968.
9. Chen Y.P., Neff P., Leske S., et al. (2025). Cochlear implantation in adults with acquired single-sided deafness improves cortical processing and comprehension of speech presented to the non-implanted ears: a longitudinal EEG study. Brain Communications. Published online 2025:fcaf001. https://doi.org/10.1093/braincomms/fcaf001
10. Neff P., Demiray B., Martin M., Röcke C. (2024). Cognitive abilities predict naturalistic speech length in older adults. Scientific Reports, 2024;14(1):31031. https://doi.org/10.1038/s41598-024-82144-w
11. Shabestari, P.S., Kleinjung, T., Schmidt, F., and **Neff, P**. (2024). Parameterized Cortical Power Spectra as a Novel Neural Feature for Real Time BCI. IEEE 12th Int. Winter Conf. Brain-Comput. Interface (BCI) 00, 1–5. https://doi.org/10.1109/bci60775.2024.10480515.
12. Sommerhalder, N., **Neff, P**., Bureš, Z., Profant, O., Kleinjung, T., and Meyer, M. (2023). Deficient central mechanisms in tinnitus: Exploring the impact on speech comprehension and executive functions. Hearing Res. 440, 108914. https://doi.org/10.1016/j.heares.2023.108914.
13. Simoes, J., Bulla, J., **Neff, P**., Pryss, R., Marcrum, S.C., Langguth, B., and Schlee, W. (2022). Daily Contributors of Tinnitus Loudness and Distress: An Ecological Momentary Assessment Study. Frontiers in Neuroscience. 16, 883665. https://doi.org/10.3389/fnins.2022.883665.
14. Basso, L., Boecking, B., **Neff, P**., Brueggemann, P., Peters, E.M.J., and Mazurek, B. (2022). Hair-cortisol and hair-BDNF as biomarkers of tinnitus loudness and distress in chronic tinnitus. Scientific Reports, 12, 1934. https://doi.org/10.1038/s41598-022-04811-0.
15. Isler, B., Burg, N. von, Kleinjung, T., Meyer, M., Stämpfli, P., Zölch, N., and **Neff, P**. (2022). Lower glutamate and GABA levels in auditory cortex of tinnitus patients: a 2D-JPRESS MR spectroscopy study. Scientific Reports, 12, 4068. https://doi.org/10.1038/s41598-022-07835-8.
16. Basso, L., Boecking, B., **Neff, P**., Brueggemann, P., El-Ahmad, L., Brasanac, J., Rose, M., Gold, S.M., and Mazurek, B. (2022). Negative Associations of Stress and Anxiety Levels With Cytotoxic and Regulatory Natural Killer Cell Frequency in Chronic Tinnitus. Frontiers in Psychology 13, 871822. https://doi.org/10.3389/fpsyg.2022.871822.
17. Basso, L., Boecking, B., **Neff, P**., Brueggemann, P., Mazurek, B., and Peters, E.M.J. (2022). Psychological Treatment Effects Unrelated to Hair-Cortisol and Hair-BDNF Levels in Chronic Tinnitus. Frontiers Psychiatry 13, 764368. https://doi.org/10.3389/fpsyt.2022.764368.

18. Schlee, W., **Neff, P**., Simoes, J., Langguth, B., Schoisswohl, S., Steinberger, H., Norman, M., Spiliopoulou, M., Schobel, J., Hannemann, R., et al. (2022). Smartphone-Guided Educational Counseling and Self-Help for Chronic Tinnitus. Journal of clinical medicine 11, 1825. https://doi.org/10.3390/jcm11071825.
19. Allgaier, J., **Neff, P**., Schlee, W., Schoisswohl, S., and Pryss, R. (2021). Deep Learning End-to-End Approach for the Prediction of Tinnitus based on EEG Data. 2021 43rd Annu. Int. Conf. IEEE Eng. Med. Biol. Soc. (EMBC) 00, 816–819. https://doi.org/10.1109/embc46164.2021.9629964.
20. Partyka, M., **Neff, P**., Bacri, T., Michels, J., Weisz, N., and Schlee, W. (2021). Gender differentiates effects of acoustic stimulation in patients with tinnitus. Prog Brain Res 263, 25–57. https://doi.org/10.1016/bs.pbr.2021.04.010.
21. Schoisswohl, S., Schecklmann, M., Langguth, B., Schlee, W., and **Neff, P**. (2021). Neurophysiological correlates of residual inhibition in tinnitus: Hints for trait-like EEG power spectra. Clinical Neurophysiology 132/7, 1694-1707. https://doi.org/10.1016/j.clinph.2021.03.038.
22. Brueggemann, P., **Neff, P**.K.A., Meyer, M., Riemer, N., Rose, M., and Mazurek, B. (2021). On the relationship between tinnitus distress, cognitive performance and aging. Prog Brain Res 262, 263–285. https://doi.org/10.1016/bs.pbr.2021.01.028.
23. **Neff, P**.K.A., Schoisswohl, S., Simoes, J., Staudinger, S., Langguth, B., Schecklmann, M., and Schlee, W. (2021). Prolonged tinnitus suppression after short-term acoustic stimulation. Prog Brain Res 262, 159–174. https://doi.org/10.1016/bs.pbr.2021.02.004.
24. **Neff, P**., Simões, J., Psatha, S., Nyamaa, A., Boecking, B., Rausch, L., Dettling-Papargyris, J., Funk, C., Brueggemann, P., and Mazurek, B. (2021). The impact of tinnitus distress on cognition. Scientific Reports 11, 2243. https://doi.org/10.1038/s41598-021-81728-0.
25. Simões, J.P., **Neff, P**.K.A., Langguth, B., Schlee, W., and Schecklmann, M. (2021). The progression of chronic tinnitus over the years. Scientific Reports 11, 4162. https://doi.org/10.1038/s41598-021-83068-5.
26. Güntensperger, D., Kleinjung, T., **Neff, P**., Thüring, C., and Meyer, M. (2020). Combining neurofeedback with source estimation: Evaluation of an sLORETA neurofeedback protocol for chronic tinnitus treatment. Restorative neurology and neuroscience 38, 283–299. https://doi.org/10.3233/rnn-200992.
27. Beierle, F., Probst, T., Allemand, M., Zimmermann, J., Pryss, R., **Neff, P**., Schlee, W., Stieger, S., and Budimir, S. (2020). Frequency and Duration of Daily Smartphone Usage in Relation to Personality Traits. Digital Psychology 1, 20–28. https://doi.org/10.24989/dp.v1i1.1821.
28. Hafner, A., Schoisswohl, S., Simoes, J., Schlee, W., Schecklmann, M., Langguth, B., and **Neff, P**. (2020). Impact of personality on acoustic tinnitus suppression and emotional reaction to stimuli sounds. Prog Brain Res 260, 187–203. https://doi.org/10.1016/bs.pbr.2020.08.004.
29. Mehdi, M., Stach, M., Riha, C., **Neff, P**., Dode, A., Pryss, R., Schlee, W., Reichert, M., and Hauck, F.J. (2020). Smartphone and Mobile Health Apps for Tinnitus: Systematic Identification, Analysis, and Assessment. JMIR mHealth and uHealth 8, e21767. https://doi.org/10.2196/21767.
30. Schlee, W., Hølleland, S., Bulla, J., Simoes, J., **Neff, P**., Schoisswohl, S., Woelflick, S., Schecklmann, M., Schiller, A., Staudinger, S., et al. (2020). The Effect of Environmental Stressors on Tinnitus: A Prospective Longitudinal Study on the Impact of the COVID-19 Pandemic. Journal of clinical medicine 9, 2756. https://doi.org/10.3390/jcm9092756.
31. Schleicher, M., Unnikrishnan, V., **Neff, P**., Simoes, J., Probst, T., Pryss, R., Schlee, W., and Spiliopoulou, M. (2020). Understanding adherence to the recording of ecological momentary assessments in the example of tinnitus monitoring. Scientific Reports 10, 1–13. https://doi.org/10.1038/s41598-020-79527-0.
32. Schoisswohl, S., Arnds, J., Schecklmann, M., Langguth, B., Schlee, W., and **Neff, P**. (2019). Amplitude Modulated Noise for Tinnitus Suppression in Tonal and Noise-Like Tinnitus. Audiology & neuro-otology 24, 309–321. https://doi.org/10.1159/000504593.
33. Simoes, J., Schlee, W., Schecklmann, M., Langguth, B., Farahmand, D., and **Neff, P**. (2019). Big Five Personality Traits are Associated with Tinnitus Improvement Over Time. Scientific Reports 9, 1–9. https://doi.org/10.1038/s41598-019-53845-4.
34. **Neff, P**., Langguth, B., Schecklmann, M., Hannemann, R., and Schlee, W. (2019). Comparing Three Established Methods for Tinnitus Pitch Matching With Respect to Reliability, Matching Duration, and Subjective Satisfaction. Trends in hearing 23, 2331216519887247. https://doi.org/10.1177/2331216519887247.
35. **Neff, P**., Zielonka, L., Meyer, M., Langguth, B., Schecklmann, M., and Schlee, W. (2019). Comparison of Amplitude Modulated Sounds and Pure Tones at the Tinnitus Frequency: Residual Tinnitus Suppression and Stimulus Evaluation. Trends in hearing 23, 2331216519833841. https://doi.org/10.1177/2331216519833841.

36. Güntensperger, D., Thüring, C., Kleinjung, T., **Neff, P**., and Meyer, M. (2019). Investigating the Efficacy of an Individualized Alpha/Delta Neurofeedback Protocol in the Treatment of Chronic Tinnitus. Neural plasticity 2019, 3540898–15. https://doi.org/10.1155/2019/3540898.
37. Simoes, J., **Neff, P**., Schoisswohl, S., Bulla, J., Schecklmann, M., Harrison, S., Vesala, M., Langguth, B., and Schlee, W. (2019). Toward Personalized Tinnitus Treatment: An Exploratory Study Based on Internet Crowdsensing. Frontiers in Public Health 7, 157. https://doi.org/10.3389/fpubh.2019.00157.
38. Beierle, F., Tran, V.T., Allemand, M., **Neff, P**., Schlee, W., Probst, T., Zimmermann, J., and Pryss, R. (2019). What data are smartphone users willing to share with researchers? Journal of Ambient Intelligence and Humanized Computing 134, 1–13. https://doi.org/10.1007/s12652-019-01355-6.
39. **Neff, P**., Hemsley, C., Kraxner, F., Weidt, S., Kleinjung, T., and Meyer, M. (2018). Active listening to tinnitus and its relation to resting state EEG activity. Neuroscience Letters 694, 176–183. https://doi.org/10.1016/j.neulet.2018.11.008.
40. Beierle, F., Tran, V.T., Allemand, M., **Neff, P**., Schlee, W., Probst, T., Pryss, R., and Zimmermann, J. (2018). Context Data Categories and Privacy Model for Mobile Data Collection Apps. Procedia Computer Science 134, 18–25. https://doi.org/10.1016/j.procs.2018.07.139.
41. Pryss, R., Probst, T., Schlee, W., Schobel, J., Langguth, B., **Neff, P**., Spiliopoulou, M., and Reichert, M. (2018). Prospective crowdsensing versus retrospective ratings of tinnitus variability and tinnitus–stress associations based on the TrackYourTinnitus mobile platform. International Journal of Data Science and Analytics 43, 1–12. https://doi.org/10.1007/s41060-018-0111-4.
42. Jagoda, L., Giroud, N., **Neff, P**., Kegel, A., Kleinjung, T., and Meyer, M. (2018). Speech perception in tinnitus is related to individual distress level - A neurophysiological study. Hearing Res 367, 48–58. https://doi.org/10.1016/j.heares.2018.07.001.
43. **Neff, P**., Michels, J., Meyer, M., Schecklmann, M., Langguth, B., and Schlee, W. (2017). 10 Hz Amplitude Modulated Sounds Induce Short-Term Tinnitus Suppression. Frontiers in Aging Neuroscience 9, 215–11. https://doi.org/10.3389/fnagi.2017.00130.
44. Meyer, M., **Neff, P**., Grest, A., Hemsley, C., Weidt, S., and Kleinjung, T. (2017). EEG oscillatory power dissociates between distress- and depression-related psychopathology in subjective tinnitus. Brain Research 1663, 194–204. https://doi.org/10.1016/j.brainres.2017.03.007.
45. Meyer, M., **Neff, P**., Liem, F., Kleinjung, T., Weidt, S., Langguth, B., and Schecklmann, M. (2016). Differential tinnitus-related neuroplastic alterations of cortical thickness and surface area. Hearing Res 342, 1–12. https://doi.org/10.1016/j.heares.2016.08.016.
46. Meyer, M., Luethi, M.S., **Neff, P**., Langer, N., and Büchi, S. (2014). Disentangling Tinnitus Distress and Tinnitus Presence by Means of EEG Power Analysis. Neural Plasticity 2014, 1–13. https://doi.org/10.1155/2014/468546.

2. Fallbeschreibungen (case reports)

3. Übersichtsarbeiten (Reviews)

1. Isler, B., **Neff, P**., and Kleinjung, T. (2023). Möglichkeiten der funktionellen Bildgebung bei Tinnitus. HNO *71*, 640–647. https://doi.org/10.1007/s00106-023-01319-5.

2. Mehdi, M., Riha, C., **Neff, P**., Dode, A., Pryss, R., Schlee, W., Reichert, M., and Hauck, F.J. (2020). Smartphone Apps in the Context of Tinnitus: Systematic Review. Sensors *20*, 1725. https://doi.org/10.3390/s20061725.

3. Schoisswohl, S., Agrawal, K., Simoes, J., **Neff, P**., Schlee, W., Langguth, B., and Schecklmann, M. (2019). RTMS parameters in tinnitus trials: a systematic review. Scientific Reports *9*, 12190–11. https://doi.org/10.1038/s41598-019-48750-9.

4. Kleinjung, T., Thüring, C., Güntensperger, D., **Neff, P.,** and Meyer, M. (2018). [Neurofeedback for the treatment of chronic tinnitus : Review and future perspectives]. HNO *66*, 198–204. https://doi.org/10.1007/s00106-017-0432-y.

5. Güntensperger, D., Thüring, C., Meyer, M., **Neff, P.,** and Kleinjung, T. (2017). Neurofeedback for Tinnitus Treatment - Review and Current Concepts. Frontiers in Aging Neuroscience *9*, 386. https://doi.org/10.3389/fnagi.2017.00386.

4. Buchbeiträge

1. **Neff, P.K.A.,** and Meyer, M. (2024). Neurofeedback. In Textbook of Tinnitus. (Springer Nature), pp. 653–666. https://doi.org/10.1007/978-3-031-35647-6_51.

2. **Neff, P.K.A.,** Shabbir, M., Goedhart, H., Vesala, M., Burns-O'Connell, G., and Hall, D.A. (2024). Public and Patient Involvement in Tinnitus Research. In Textbook of Tinnitus. (Springer Nature), pp. 717–729. https://doi.org/10.1007/978-3-031-35647-6_56.

3. Schlee, W., Kraft, R., Schobel, J., Langguth, B., Probst, T., **Neff, P**., Reichert, M., and Pryss, R. (2019). Momentary Assessment of Tinnitus—How Smart Mobile Applications Advance Our Understanding of Tinnitus. In Studies in Neuroscience, Psychology and Behavioral Economics. New Developments in Psychoinformatics., H. B. C. Montag and C. Montag, eds. (Springer), pp. 209–220. https://doi.org/10.1007/978-3-030-31620-4_13.

5. Monographien

6. Angeleitete Dissertationen

7. Sonstige wissenschaftliche Publikationen, die als wichtig erachtet werden

1. Simões J.P., Klooster P., **Neff P.K.**, Niemann U., Kraiss J. (2024). Editorial: Artificial intelligence and mental health care. Front Public Heal. 2024;12:1461446. https://doi.org/10.3389/fpubh.2024.1461446 (Editorial)

2. Cederroth, C.R., Kleinjung, T., Langguth, B., Noreña, A., **Neff, P**., Mazurek, B., Dijk, P.V., and Schlee, W. (2024). Editorial: Towards an understanding of tinnitus heterogeneity, volume II. Frontiers in Aging Neuroscience. *16*, 1376600. https://doi.org/10.3389/fnagi.2024.1376600. (Editorial)

3. Kleinjung, T., Meyer, M., and **Neff, P**. (2023). Neurofeedback for tinnitus treatment: an innovative method with promising potential. Brain Commun. *5*, fcad209. https://doi.org/10.1093/braincomms/fcad209. (Perspective)

4. Simoes, J.P., Schoisswohl, S., Schlee, W., Basso, L., Bernal-Robledano, A., Boecking, B., Cima, R., Denys, S., Engelke, M., Escalera-Balsera, A.,….**Neff, P**… et al. (2023). The statistical analysis plan for the unification of treatments and interventions for tinnitus patients randomized clinical trial (UNITI-RCT). Trials *24*, 472. https://doi.org/10.1186/s13063-023-07303-2. (Protocol)

5. Martins, M.L., Kleinjung, T., Meyer, M., Raveenthiran, V., Wellauer, Z., Peter, N., and **Neff, P.** (2022). Transcranial electric and acoustic stimulation for tinnitus: study protocol for a randomized double-blind controlled trial assessing the influence of combined transcranial random noise and acoustic stimulation on tinnitus loudness and distress. Trials *23*, 418. https://doi.org/10.1186/s13063-022-06253-5. (Protocol)

6. Ridder, D.D., Schlee, W., Vanneste, S., Londero, A., Weisz, N., Kleinjung, T., Shekhawat, G.S., Elgoyhen, A.B., Song, J.-J., Andersson, G., … **Neff, P.,**… et al. (2021). Tinnitus and tinnitus disorder: Theoretical and operational definitions (an international multidisciplinary proposal). Prog Brain Res *260*, 1–25. https://doi.org/10.1016/bs.pbr.2020.12.002. (Perspective)

7. Schlee, W., Schoisswohl, S., Staudinger, S., Schiller, A., Lehner, A., Langguth, B., Schecklmann, M., Simoes, J., **Neff, P**., Marcrum, S.C. and Spiliopoulou, M., 2021. Towards a unification of treatments and interventions for tinnitus patients: The EU research and innovation action UNITI. Prog Brain Res, *260*, pp.441-451.https://doi.org/10.1016/bs.pbr.2020.12.005. (Project description)

8. Schoisswohl, S., Langguth, B., Schecklmann, M., Bernal-Robledano, A., Boecking, B., Cederroth, C.R., Chalanouli, D., Cima, R., Denys, S., Dettling-Papargyris, J., …**Neff, P**.,… et al. (2021). Unification of Treatments and Interventions for Tinnitus Patients (UNITI): a study protocol for a multi-center randomized clinical trial. Trials *22*, 875. https://doi.org/10.1186/s13063-021-05835-z. (Protocol)

9. Pryss, R., Schlee, W., Reichert, M., Kurthen, I., Giroud, N., Jagoda, L., Neuschwander, P., Meyer, M., **Neff, P.,** Schobel, J., et al. (2019). Ecological Momentary Assessment based Differences between Android and iOS Users of the TrackYourHearing mHealth Crowdsensing Platform. In 41st Annual International Conference of the IEEE Engineering in Medicine and Biology Society (EMBC)., pp. 3951–3955. https://doi.org/10.1109/embc.2019.8857854. (Conference)

10. **Neff, P.,** Bisig, D., and Schacher, J.C. (2019). State Dependency - Audiovisual interaction through brain states. Sound and Music Computing (SMC) Conference, pp. 1–8. https://smc2019.uma.es/articles/P1/P1_04_SMC2019_paper.pdf. (Conference)

11. Beierle, F., Tran, V.T., Allemand, M., **Neff, P.,** Schlee, W., Probst, T., Pryss, R., and Zimmermann, J. (2018). TYDR – Track Your Daily Routine. Android App for Tracking Smartphone Sensor and Usage Data. In the 5th International Conference., pp. 72–75. https://doi.org/10.1145/3197231.3197235. (Conference)

12. Pryss, R., Probst, T., Schlee, W., Schobel, J., Langguth, B., **Neff, P.,** Spiliopoulou, M., and Reichert, M. (2017). Mobile Crowdsensing for the Juxtaposition of Realtime Assessments and Retrospective Reporting for Neuropsychiatric Symptoms. 2017 IEEE 30th Int. Symp. Comput.-Based Med. Syst. (CBMS), 642–647. https://doi.org/10.1109/cbms.2017.100. (Conference)

13. Schacher, J.C., and **Neff, P.** (2016). Skill development and stabilisation of expertise for electronic music performance. Music, Mind, and Embodiment. CMMR 2015. Lecture Notes in Computer Science. *9617*, 111–131. https://doi.org/10.1007/978-3-319-46282-0_7. (Conference)

14. Schacher, J.C., Strinning, H.J.C., Strinning, C., and **Neff, P.** (2015). Movement perception in music performance-a mixed methods investigation. Proceedigs of the International Conference on Sound and Music Computing. 10.5281/ZENODO.851106. (Conference)

15. Serquera, J., Schlee, W., Pryss, R., **Neff, P.,** and Langguth, B. (2015). Music Technology for Tinnitus Treatment Within Tinnet. Proceedings of 58th International AES Conference: Music Induced Hearing Disorders. https://aes2.org/publications/elibrary-page/?id=17783. (Conference)

scientific reports

Check for updates

OPEN

Prediction of acoustic tinnitus suppression using resting-state EEG via explainable AI approach

Payam S. Shabestari[1], Stefan Schoisswohl[2,3], Zino Wellauer[4], Adrian Naas[5,6], Tobias Kleinjung[1], Martin Schecklmann[2], Berthold Langguth[2] & Patrick Neff[1,2]✉

Tinnitus is defined as the perception of sound without an external source. Its perceptual suppression or on/off states remain poorly understood. This study investigates neural traits linked to brief acoustic tinnitus suppression (BATS) using naive resting-state EEG (closed eyes) from 102 individuals. A set of EEG features (band power, entropy, aperiodic slope and offset of the EEG spectrum, and connectivity) and standard classifiers were applied achieving consistent high accuracy across data splits: 98% for sensor and 86% for source models. The Random Forest model outperformed other classifiers by excelling in robustness and reduction of overfitting. It identified several key EEG features, most prominently alpha and gamma frequency band power. Gamma power was stronger in the left auditory network, while alpha power dominated the right hemisphere. Aperiodic features were normalized in individuals with BATS. Additionally, hyperconnected auditory-limbic networks in BATS suggest sensory gating may aid suppression. These findings demonstrate robust classification of BATS status, revealing distinct neural traits between tinnitus subpopulations. Our work emphasizes the role of neural mechanisms in predicting and managing tinnitus suppression. Moreover, it advances the understanding of effective feature selection, model choice, and validation strategies for analyzing clinical neurophysiological data in general.

Chronic subjective tinnitus is defined as the persistent and conscious auditory perception of tonal or composite noise in the absence of an equivalent external physical acoustic source, which can evolve into a more complex syndrome termed 'tinnitus disorder' marked by high levels of tinnitus-related distress [1,2]. With a prevalence of about 14.4%, tinnitus is a common condition in the global population with many of those affected experiencing severe burden [3], and suffer from several comorbidities such as depression or anxiety disorders [4]. Currently, no effective treatment for tinnitus is established or on the horizon and the available treatment approaches only focus on secondary symptoms such as quality of life management [5–7]. Typically, tinnitus is thought to evolve as a consequence of noise trauma and/or hearing loss[8], whereby the resulting lack of peripheral auditory input provokes maladaptive pathological changes in the auditory pathway as well as the central nervous system putatively responsible for the perception of the auditory phantom sound perception tinnitus [9–11]. These pathological alterations further translate into distinctive tinnitus-related spontaneous brain activity patterns; here, increased activity in the delta and gamma frequency bands and decreased activity in the alpha frequency band in (sensory) auditory cortical regions have been reported by electroencephalography (EEG) or magnetoencephalography (MEG) by several research groups [12–15]. Moreover, tinnitus-related alterations in functional global and modality-specific networks have been reported [16]. Generally, these alterations include increased connectivity within and between the auditory network, the default mode network, the attention networks, and the visual network.

In past studies, various machine learning approaches were applied to differentiate the tinnitus population from healthy controls using resting state EEG data with high accuracy [17–20]. However, to this day, machine learning studies concerning active manipulation of tinnitus have not been carried-out within the tinnitus population.

A large portion of individuals with tinnitus (60-80%) are capable of undergoing temporary suppression of the subjective tinnitus perception to some degree following sound stimulation with either white noise, sine tones, or various (complex) modulated or filtered stimuli [21–27]. Brief Acoustic Tinnitus Suppression (BATS),

[1]Department of Otorhinolaryngology, Head and Neck Surgery, University Hospital Zurich, University of Zurich, Zurich, Switzerland. [2]Department of Psychiatry and Psychotherapy, University of Regensburg, Regensburg, Germany. [3]Department of Psychology, Universitaet der Bundeswehr München, Neubiberg, Germany. [4]Department of Comparative Language Science, University of Zurich, Zurich, Switzerland. [5]Business School, Institute New Work, Bern University of Applied Sciences, Bern, Switzerland. [6]Department of Psychology, University of Fribourg/Freiburg, Fribourg/Freiburg, Switzerland. ✉email: patrick.neff@uzh.ch

established as "residual inhibition" or "forward masking"[28,29], is theorized to result from a temporary recovery of imbalanced inhibitory and excitatory neuronal activity in the auditory cortex and/or reduced firing of neurons along the auditory pathway [30]. While studying the subcortical auditory pathway below the brainstem in human participants is challenging, so far only three studies focused on cortical activity related to BATS on a group level, besides three single case studies showing heterogeneous findings [31–33]: Kahlbrock and Weisz [34] observed a decline in pathologically enhanced activity in the delta frequency range, whereas King and colleagues's study indicated elevated power spectral density concerning gamma and alpha activity [35]. Similarly, we could demonstrate in our former study [36] that participants who experience BATS had enhanced alpha activity in general compared to participants without BATS. In contrast to King and colleagues' study, however, we observed reduced gamma band amplitudes. This observation further emphasizes specific oscillatory signatures of tinnitus patient subtypes related to the ability to induce short-term tinnitus suppression via acoustic stimulation. Currently, there seems to be convergence regarding the role of alpha in BATS with most studies reporting an increase while in other frequency bands, especially gamma, the results are diverging and partly contradicting.

To the best of our knowledge, no former study attempted to predict tinnitus suppression, 'off-states', or specifically BATS from (naive) resting state M/EEG data. In contrast to former studies in BATS probing short-term state-like neural responses during BATS or classification thereof, this approach may elucidate how individual trait-like or phenotypic neural signatures influence the ability to suppress tinnitus. We therefore consider elaboration on trait-specific (oscillatory) brain activity patterns associated with BATS to be of high interest, given the potential to accurately identify individuals with the ability to acoustically suppress their tinnitus. Such accurate classifiers could in turn be of use in tinnitus subtyping, objective diagnosis, and early identification of individual treatment options like sound therapies [37]. Automatic, high-accuracy classification and insights gained from resulting, distinctive features would enable us to better understand the BATS phenomenon and basic mechanisms of tinnitus on the neural level including neuroplasticity. Explainable AI has the potential to surpass traditional analysis methods by enabling a comprehensive examination of models and important features [38]. Furthermore, this approach could foster (objective) diagnostic options, tinnitus subtyping, and identification of individual treatment options like sound therapies [37]. Related to that, it was recently shown that certain EEG features such as frequency band power and functional connectivity could predict treatment response to a sound-based intervention with 98-100% accuracy [39].

Currently, it remains unclear which trait-like factors or signatures of (oscillatory) brain activity and connectivity can predict BATS. Hence, the objective of the present work is to apply automatic classification algorithms to evaluate if distinctive EEG sensor, source, and connectivity features are predictive of BATS.

Materials and methods

Data sets

The EEG and behavioral data used in this study were sourced from two distinct labs at the universities of Regensburg, Germany, and Zurich, Switzerland. The Regensburg dataset encompassed 79 participants who actively participated in two neurobehavioral experiments investigating BATS with EEG. These experiments received ethical approval from the internal ethics review board of the Faculty of Medicine, Regensburg, under reference numbers 17-819-101 and 18-1054-101. The Zurich validation set consisted of 29 participants partaking in a neuromodulation study where EEG and BATS were assessed during baseline measurements. Ethical approval for the Zurich study was obtained from the Cantonal Ethics Committee (KEK, Zurich; BASEC-Nr. 2020-02027). All individuals included in the studies pertaining to the dataset at hand provided informed consent for both their participation in the studies and the utilization of their data for future analyses. The experiments were conducted in strict compliance with the ethical principles outlined in the Declaration of Helsinki.

For more comprehensive details and descriptive statistics related to the data sets, readers are referred to the supplementary material tables S1 and S2.

Feature extraction

An overview of our method pipeline is shown in Fig 1. Following the preprocessing and epoching of the EEG data, a set of frequency domain features, comprising oscillatory power estimation, non-oscillatory parameters, and information measures, was extracted for each EEG epoch, with calculations performed individually at the level of each electrode and brain region. The features computed per electrode consisted of: Sensor space spectral power values averaged within the five canonical M/EEG frequency bands (comprising 310 features), average spectral Shannon entropy (comprising 310 features) [40,41], and non-oscillatory parameters, such as the slope and offset of power spectral density at each electrode (comprising 124 features) [42]. Entropy measures the complexity or unpredictability of brain activity, providing insights into neural dynamics and cognitive states. Higher entropy typically reflects more complex, less predictable signals, while lower entropy suggests more regular, structured activity [43,44]. (see supplemental information for details.) For each designated brain region extracted from Desikan-Killiany [45] atlas (source space), the features computed encompass the average spectral power across five distinct frequency bands within the epochs (comprising 340 features). See the supplementary section for a detailed explanation of how each feature set was computed. The (standard) frequency bands utilized for computing features encompass: Delta (0.5-4.5 Hz), Theta (4.5-8.5 Hz), Alpha (8.5-13.5 Hz), Beta (15-30 Hz) and Gamma (30–80 Hz) [46].

Due to the intrinsic correlation between spectral power values in the sensor space and source space, we divided the features into two distinct sets. Feature set 1, which pertains to the sensor space, was employed to explore the significance and direction of spectral power and spectral entropy in canonical frequency bands, as well as non-oscillatory activity in predicting BATS. By exploiting the classification results of feature set 1, it was narrowed-down into feature set 2 in source space, focusing solely on spectral power values associated with brain

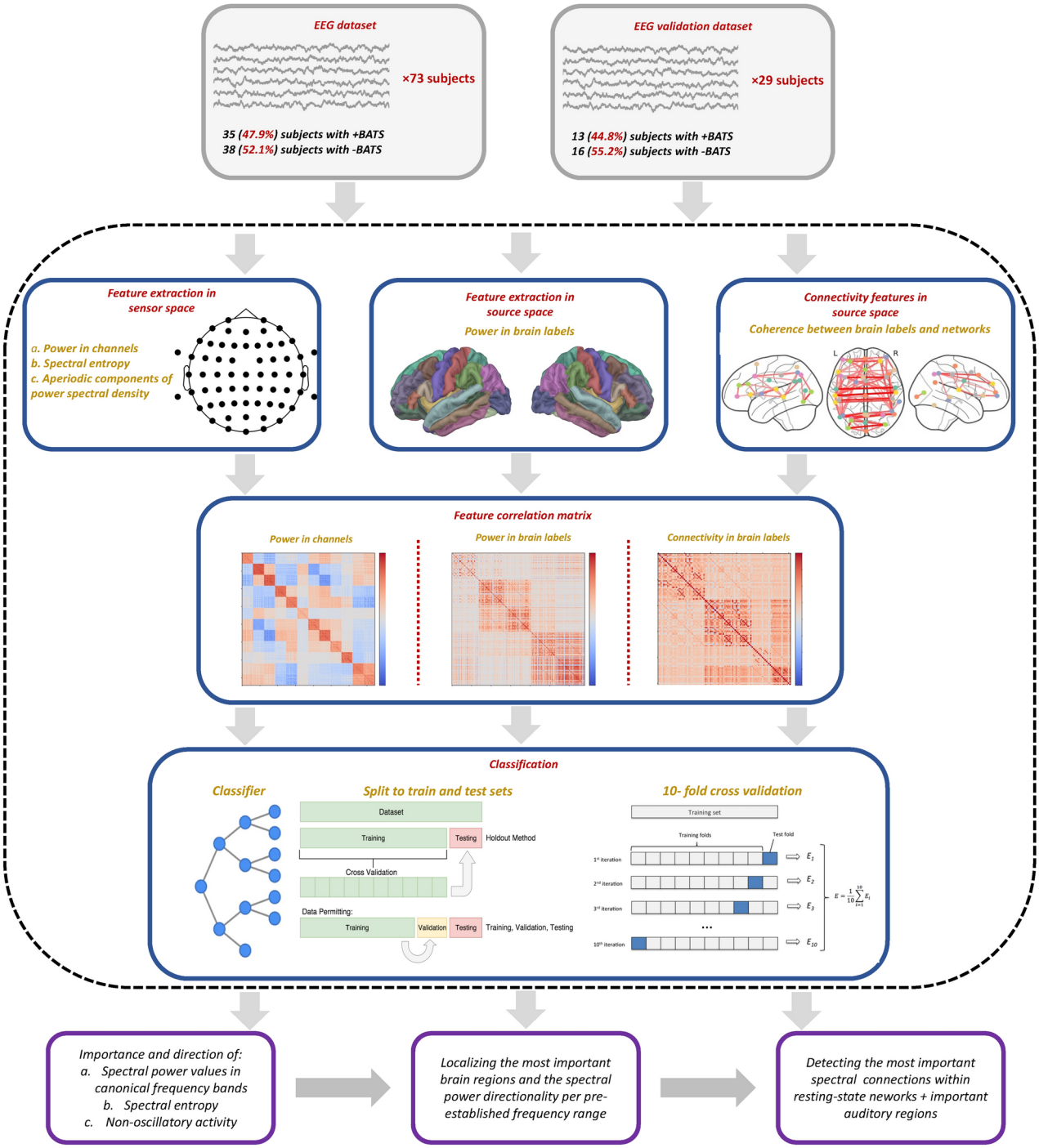

Fig. 1. Overview of the analysis pipeline. EEG data collected from 73 participants (main dataset) was divided into 2-second epochs after preprocessing. Sensor space features with high correlation were merged using Pearson correlation. Data was partitioned into training and test sets, and a 10-fold cross-validation was performed on the training set. Further analysis involved ranking features based on their importance and exploring their directional impact. A parallel process was applied to the epochs using features computed in the source space. The outcomes of these analyses were utilized to calculate spectral connectivity features in each frequency band and between brain regions (labels) in the source space. Furthermore, all procedures were performed on an additional, independent EEG dataset of 29 participants to validate and benchmark the results.

regions. This procedure will help to investigate the specific contribution of individual brain regions (or labels) in the prediction of BATS.

Further, coherence metrics across frequency bands and brain regions identified as important through source space analysis were computed. Coherence, quantifies the functional connectivity between different brain

regions by measuring the consistency of phase relationships across frequencies. It is commonly used to assess neural synchronization, with higher coherence indicating stronger communication between regions. (refer to supplementary materials for more details). For the analysis of functional connectivity patterns across different resting-state brain networks, the Desikan-Killiany atlas was utilized [45] and brain regions were organized into networks as delineated in the supplementary Table S3. Seven large-scale functionally segregated networks [47,48] were categorized, including visual (VSN), somatomotor (SMN), dorsal attention (DAN), ventral attention (VAN), limbic (LBN), frontoparietal (FPN), and default mode (DMN) networks. Recognizing the particular importance of the auditory network (AUN) in tinnitus, we incorporated nine distinct sub-networks along with most contributing brain regions detected within the AUN network. Labels for the left or right hemisphere were included if the corresponding label in the other hemisphere was missing to account for the brain's bi-hemispheric functional organization.

Classification pipeline

Features with correlation coefficients exceeding 0.9 were merged using Pearson correlation. A threshold of 0.9 is commonly used to ensure that remaining features are sufficiently distinct to contribute unique information to the model [49]. The selected set of features significantly improved the model's interpretability and its ability to generalize across different datasets. Then, the classification process was performed by shuffling the epochs and then randomly splitting them into a 70% training and a 30% test set. Following this initial split, a 10-fold cross-validation procedure was carried-out exclusively on the training set, and finally, the classification algorithm's accuracy was computed using the test set as follows:

$$\text{accuracy} = \frac{\#TP}{\#TP + \#FN + \#FP} \tag{1}$$

where $\#TP$ represents the count of true positives, signifying correctly classified epochs from individuals with BATS. $\#FN$ corresponds to the count of false negatives, encompassing misclassified epochs from individuals with +BATS, and $\#FP$ denotes the count of false positives, including individuals incapable of persistently suppressing tinnitus (-BATS) but have been incorrectly assigned to the other class. In our analysis, we employed 10 widely recognized classifiers from the `scikit-learn` python package [50] with their respective default parameters. These classifiers comprise: Random Forest (RF) [51], Gradient Boosting [52], Quadratic Discriminant Analysis (QDA) [53], Naive Bayes [54], Decision Tree [55], Radial Basis Function (RBF) kernel SVM [56], Gaussian Process [57], k-nearest neighbors [58], Convolutional Neural Network [59] and linear SVM [60]. By utilizing such a diverse set of classifiers, it was evaluated if the classification task is robust across classifiers and the different thresholds for BATS.

After benchmarking the set of classifiers, the best performing model was selected and subjugated to feature importance analysis. Feature importance was determined based on the mean and standard deviation of the reduction in impurity within each tree, known as Gini impurity metric (see supplementary materials). Subsequently, we retrained the model, using only the top 100 features identified through this process. To assess the significance and directional impact of features (sensor space, source space, or spectral connections) in predicting the two classes (i.e., +BATS and -BATS), we utilized the `SHAP` (SHapley Additive exPlanations) Python package [61].

Validation

To validate and benchmark our results, we utilized a distinct validation dataset, which is detailed in the "Data sets" section. The same methodology as detailed in section "Feature extraction" and "Classification pipeline" was applied to the validation dataset, including the computation of predefined feature sets both in the sensor and source space as well as spectral connectivity measures. For classification, a BATS threshold of -1 was employed to categorize participants into two groups: those who did show acoustical suppression of their tinnitus (with values less than or equal to -1) and those who did not (with values larger than -1). Note, the scale ranged from 0 indicating no suppression to -5 indicating full suppression. Moreover, we computed models where the BATS labels (i.e., +BATS and -BATS) of the data split were randomly shuffled so each label consisted of a mixture of true and false labels (50% mixture). This allowed for validation of our models and the related ground truth assumption, namely, the ability to suppress tinnitus based on individuals' self-reports.

Results

Sensor space

As a result of the feature correlation check, 92 features, which accounted for 12.4% of the original 744, were excluded due to their high correlation. We furthermore assessed the accuracy of our models on test data by setting the BATS threshold to five different values (here: perceived tinnitus loudness during +BATS): 90, 80, 70, 60, and 50. For consistency in subsequent classification tasks conducted in the source space and connectivity analysis, we adopted RF as our standard classifier and set the threshold for +BATS to 90 (see "Discussion" for more details). Notably, our ancillary randomly-shuffled label models analysis for this threshold resulted in an accuracy of 51.7% for the RF model, providing clear evidence for the feasibility of our choice of ground truth in this analysis. After selecting the top 100 most important features and retraining the model, we achieved an accuracy of 98.6% for the RF model on the test data.

Subsequently, by assessing the importance of these features, we discovered that the power spectrum averaged over the gamma and alpha frequency bands exerted the most significant influence on the model's predictions for both classes, namely +BATS and -BATS, as depicted in Fig. 3A. Investigating the directional impact of these features, we observed that spectral power values in the gamma frequency range had a bidirectional effect on

predicting both classes, with a tendency of high gamma feature values predicting +BATS. Moreover, higher alpha feature values apparently exert a more significant impact on predicting individuals with +BATS, suggesting that individuals with tinnitus who show higher alpha activity during an independent EEG resting-state measurement are more likely to successfully show inhibition of their tinnitus. Channels identified as important contributors by the classification are depicted in Fig. 3B and mostly covering auditory, sensory, and/or attentional networks. Yet, given well-known issues of volume conduction, diffusion, and smearing in M/EEG sensor level localization, source-localized data, as presented in the next section, is more feasible for further interpretation. Entropy values were calculated in order to extend the assessment of power values by contributing measures of orderliness or informational value. Looking at the impact on the model output (SHAP values) in Fig. 3A, D, entropy feature values confirm the bidirectional outcome for gamma and the positive influence of alpha power on tinnitus suppression by showing an inversion of the distribution of the power effects. Furthermore, power values in alpha and gamma are negatively correlated, shown in Fig. 3D in the right-most subplot. Finally, aperiodic parameters complement the results of the feature set showing that +BATS is related to lower aperiodic offsets and steeper slopes (resulting in a larger area under the curve), which reflects more periodic (i.e., oscillatory) activity or 'normal' power frequency spectrum in individuals with +BATS (Fig. 3C).

Source space

Following the merging of features with high correlation, a total of 263 features, constituting 77% of the original 340, were excluded from our dataset. Subsequently, we trained the model and classified the data using these refined features, resulting in an accuracy of 97.8% for the RF model on the test data. Examining the overall importance of spectral power values within different frequency bands across brain labels indicated that delta, theta, and beta oscillations accounted for 10.3%, 13.3%, and 19.2% of the total feature importance, respectively. However, alpha and gamma oscillations contributed substantially more significantly, making up 27.2% and 29.8% of the total feature importance. This importance order aligns with results from the classification process performed in sensor space features. Figure 4 displays the key brain labels that contribute the most to the classification task, along with their predictive direction. The source model extends the findings of sensor space locations in the previous model by confining features to functionally-segregated brain regions. In general, alpha power was more pronounced in the right brain hemisphere whereas gamma power seems to exert a bias to the left hemisphere (Fig. 4A, B), at least regarding temporal and (primary) auditory fields. Furthermore, identified labels in primary auditory regions (transverse temporal, middle temporal) extend to non-auditory regions associated with sensory integration (superior parietal, supramarginal, precentral and paracentral), executive and attentional control (superior frontal, frontal pole), memory (parahippocampal, posterior cingulate), and limbic emotional (interface) integration (insula, rostral anterior cingulate, and temporal pole), for alpha and gamma, respectively. In the insula, high alpha power is not predictive of +BATS, whereas the opposite pattern can be observed for alpha power in the rostral anterior and the posterior cingulate cortex, and superior frontal gyrus. In the remaining labels of the alpha band, the impact on the model's output is bidirectional or mixed. Gamma power is predictive of +BATS in (left) transverse temporal gyrus, rostral anterior cingulate cortex, and paracentral gyrus whereas it is not predictive in superior parietal and supramarginal gyri. For the remaining labels in gamma, their influence on the model's output is observed to be bidirectional or variable.

Connectivity

We calculated the coherence connectivity measure within the resting state network's brain labels and between the important brain labels identified in the source space analysis. The coherence measures were computed for each epoch, and 20 features out of 102 features were excluded due to high correlations (19.6%). Consequently, the training phase involved 82 features, encompassing connections between resting state networks and auditory network brain labels within two frequency ranges, specifically alpha and gamma. After training the model, we achieved an accuracy of 86.3%. The most important connections for both frequency ranges are presented in Fig. 5. Overall, the predictive feature set of this model is driven by important gamma connections between several networks and nodes while important connectivity in the alpha frequency band was limited to 3 between-network connections and 2 intra-auditory network connections (hyperconnectivity between bilateral primary auditory fields in superior and transverse temporal gyrus as well as superior parietal gyrus. Interestingly, all alpha between-network connections (i.e., VAN and DMN or DGN, AUN and DAN) were not predictive of +BATS indicating a global and trait-like decoupling of these networks +BATS individuals. In contrast, intra-auditory network connections in the alpha band (i.e., between superior temporal, parietal, and transverse temporal gyri) are predictive of +BATS. Gamma connectivity predictive of +BATS resulted between AUN and SMN, AUN and LBN, AUN and DGN, SMN and FPN, and VAN and DAN, while the remaining connectivity features had mixed or negative impact on the model output (i.e., VAN and DGN, AUN and FPN, VAN and LBN, and VAN and SMN). Finally, a single intra-auditory network connection in the gamma frequency band predictive of +BATS was found between left superiorparietal gyrus and right superiortemporal gyrus.

Behavioral data

In the analysis of behavioral data of the main dataset, statistically significant higher Minimum Masking Levels (MML) were observed in the -BATS group compared to the +BATS group. This result indicates a potential correlation between the ability to acoustically suppress tinnitus and the MML (mean difference = 7.63 dB, supplementary Table S2). Additionally, while not reaching the level of statistical significance, there was a trend towards higher tinnitus loudness levels in the -BATS group (mean difference = 8.58 dB), which is in line with the MML finding and suggests a relationship between tinnitus maskability during sound presentation and residual inhibition after sound presentation.

Validation

We conducted an ancillary analysis using a validation dataset to assess the generalizability of our findings and whether the identified important brain labels were consistent across different recording systems and varied levels of +BATS obtained from different response scales (see supplementary Figs. S1, S2 and S3. Spectral power values were computed in brain parcels, following the same methodology outlined in "Feature extraction" section. Feature merging was performed to address high correlations, resulting in 107 (68.5%) features being retained from the initial 340 features and data classification was carried out in the sensor space, using the remaining features with a selected loudness threshold value of −1. An RF model was employed, and an accuracy of 99.1% was achieved on the test data, using the top 100 most important features. When comparing the important brain labels obtained from the validation dataset analysis with the top 10 most important brain labels from the main dataset, we observed that in the alpha frequency range, 7 out of the 10 brain labels were important in both datasets. The 3 non-overlapping brain labels were the paracentral gyrus, insula, and posterior cingulate. Notably, the reason for their absence in the validation set was the presence of high correlations with other brain parcels, which led to their removal in the initial feature merging step. Specifically, the paracentral gyrus exhibited high correlation with labels: postcentral, posterior cingulate, superior parietal, and supramarginal. The insula displayed high correlation with brain labels: lateral orbitofrontal, medial orbitofrontal, pars opercularis, pars orbitalis, pars triangularis, rostral middle frontal, and superior temporal, and the posterior cingulate was removed due to its high correlation with the supramarginal label. In the gamma frequency range, 7 out of the 10 most important brain labels matched between the two datasets. Similarly, 3 out of the 10 brain labels did not appear in the validation dataset. These were the rostral anterior cingulate (due to high correlation with superiortemporal and temporal pole), paracentral (due to high correlation with postcentral, posterior cingulate, superior parietal, and supramarginal), and superior parietal (due to high correlation with supramarginal).

Finally, we conducted training and testing of a RF model on the validation data using connectivity features computed as described in Section "Feature extraction". This analysis resulted in an accuracy of 82.2%. When we compared the most important connections derived from the main dataset with those from the validation dataset, we found that most of the important connections were present in the validation dataset's results, while both the order and the extent of the feature list vary considerably. In general, considering that there is a 70% match between the important brain labels in both the alpha and gamma frequency ranges and taking into account that the remaining labels were dropped due to the feature merging process, we can conclude that the validation dataset successfully validated the findings from the main dataset. This level of consistency supports the robustness and reliability of our results across different datasets and recording systems.

Discussion

In the present study, we aimed to ascertain if specific sensor, source, or connectivity features of resting state EEG from individuals with tinnitus predict tinnitus suppression by auditory stimulation. We showed that high classification accuracy can be found for several BATS threshold levels (split validation) and in an independent dataset. Important neural features were identified and subjected to model impact and directionality (of effects) analysis, which resulted in specific patterns of neural signatures aligning and extending current models of tinnitus. In the absence of any directly comparable previous work (i.e., prediction of acoustic tinnitus suppression from naive (EEG) resting state data and not by experimental state-like BATS data), referential discussion within the tinnitus literature in the following section is inherently limited. We first discuss the classification workflow and results, followed by an integrative discussion of resulted neural features with respect to tinnitus and general brain models following the sequence of analysis steps (see Fig. 1). Limitations, future directions, and the conclusion will finally complement the discussion.

Classification

Our analysis demonstrated the feasibility of robustly classifying individuals with regards to acoustically-induced tinnitus suppression based on naive EEG resting state recordings. We demonstrated that the classification task remains robust and consistently yields high accuracy on unseen data for various BATS threshold values (see Fig. 2). After removing highly correlated features (> 0.9), the models achieved high accuracy values on test data, suggesting that the high accuracy is not due to overfitting. This level of performance indicates that the model has learned meaningful patterns from the data rather than memorizing noise or redundant information, as validated by its strong generalization to unseen test samples. This was further confirmed by our ancillary randomly-shuffled label model analysis, which resulted in almost chance-level accuracy (51.7%). In contrast to classical approaches that focus primarily on designing classifiers, even complex ones, to achieve high accuracy without a deep exploration of the underlying dynamics, the emphasis of this work is distinct: The focus lies not in classification per se, but in meaningful, explainable outcomes that foster the understanding of the underlying patterns. Showing that various simple models consistently yield high classification accuracy implies that the problem inherently possesses a global minimum in the parameter space for all classifiers. This implies that various simple models converge to the same optimal solution, indicating robustness and reliability across different approaches to classification. Beyond that, we assessed the importance and directionality of the feature classes for different loudness threshold levels, as illustrated in supplementary Figure S1. This ancillary analysis further highlighted consistency in both importance and direction across the class of features. Any (usually small) variations observed may be mostly attributed to the random selection of training and test sets, shuffling or data imbalance. This suggests that the choice of the threshold does not strongly influence the data's underlying pattern. This robustness indicates that the features have been well-designed and offer clear separability between the two classes, resulting in consistent model performance across different thresholds. The ultimate choice of a 10% BATS threshold (tinnitus loudness threshold at 90% after stimulation) for the main analysis is thus solely

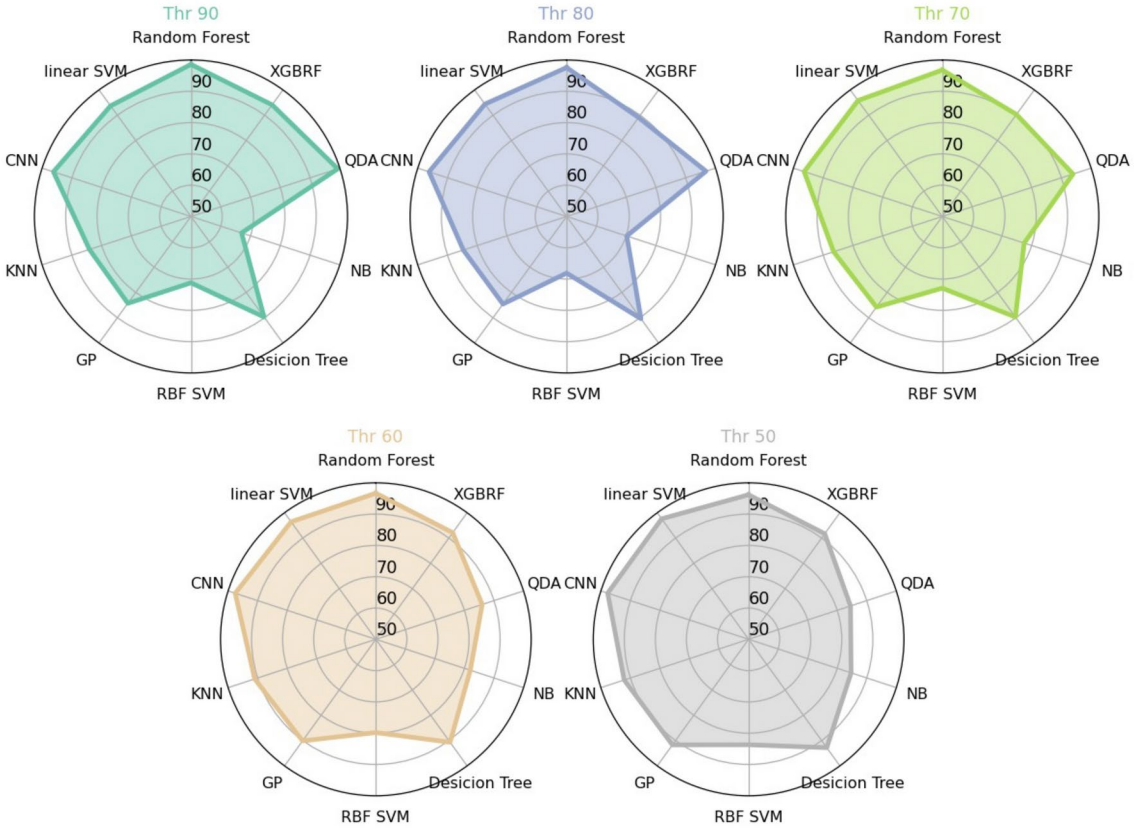

Fig. 2. Performance of the classifiers. The performance (accuracy) of ten distinct classifiers was visualized on 2-second EEG epochs, consisting of 10,332 data points and 652 features in sensor space. The classifiers applied included RF, XGBRF, QDA, NB, Decision Tree, RBF SVM, GP, KNN, CNN, and linear SVM, with varying BATS thresholds from 90 to 50, in steps of 10 (represented by different circles). Accuracy values ranged from 50% (chance level) at the center of the circles to 100% (perfect prediction) at the circumference of the circles. We selected the Random Forest classifier as the best performer due to its robust performance across different threshold levels and its optimal performance at the 90% threshold compared to the other classifiers.

motivated to create a balanced dataset. This threshold results in a distribution where 47.9% of individuals have +BATS, and 52.1% have -BATS, which ultimately reduces model bias and leads to fairer predictions.

Since preserving the inherent meaning of our features is important, we did not employ advanced feature selection or reduction techniques like PCA [62] or NCA [63], which involve linear combinations of features. We instead utilized Pearson correlation approach to merge features that exhibit high correlations to address the issue of multicollinearity in our dataset while keeping features interpretable. This process reduced dataset dimensionality, eliminated multicollinearity, and mitigated overfitting, retaining essential data for classification. However, features that exhibit a non-linear connection may be retained despite potentially showing a weak Pearson correlation, as the Pearson correlation specifically assesses linear associations. Merging such features based on correlation could be detrimental in certain configurations. Moreover, choosing the wrong threshold for merging the features can lead to either under-merging (retaining too many features) or over-merging (losing important information).

We ultimately selected the RF model to classify individuals with respect to their ability to suppress their tinnitus for several reasons: First, its majority voting mechanism naturally mitigates the risk of overfitting and helps lower variance error, promoting more robust and reliable predictions [51] (see supplementary Table S4). Second, RF is known for being less sensitive to hyperparameter choices compared to other models. Third, it offers a measure of feature importance through the Gini impurity metric [64]. Additionally, it consistently demonstrated superior performance across various loudness thresholds, further validating its suitability for the task. Lastly, RF is an ensemble which is helpful if unbalanced data is present, in contrast to other classifier methods. Therefore, its inclusion and application on different BATS splits can be considered as optimal.

Features with low importance may have limited impact on the model's predictive capabilities and can potentially be removed to simplify the interpretation of the model. On the other hand, if feasible and of interest, one could consider their effect on the model's output as well. As an example, when examining non-oscillatory features of power spectrum density, including PSD offset and slope, we observed that as moving towards lower offset values and higher slope values (indicating reduced aperiodic activity), the model tends to predict the class of individuals who consistently showed tinnitus suppression (+BATS). This relationship is illustrated in Fig. 3C.

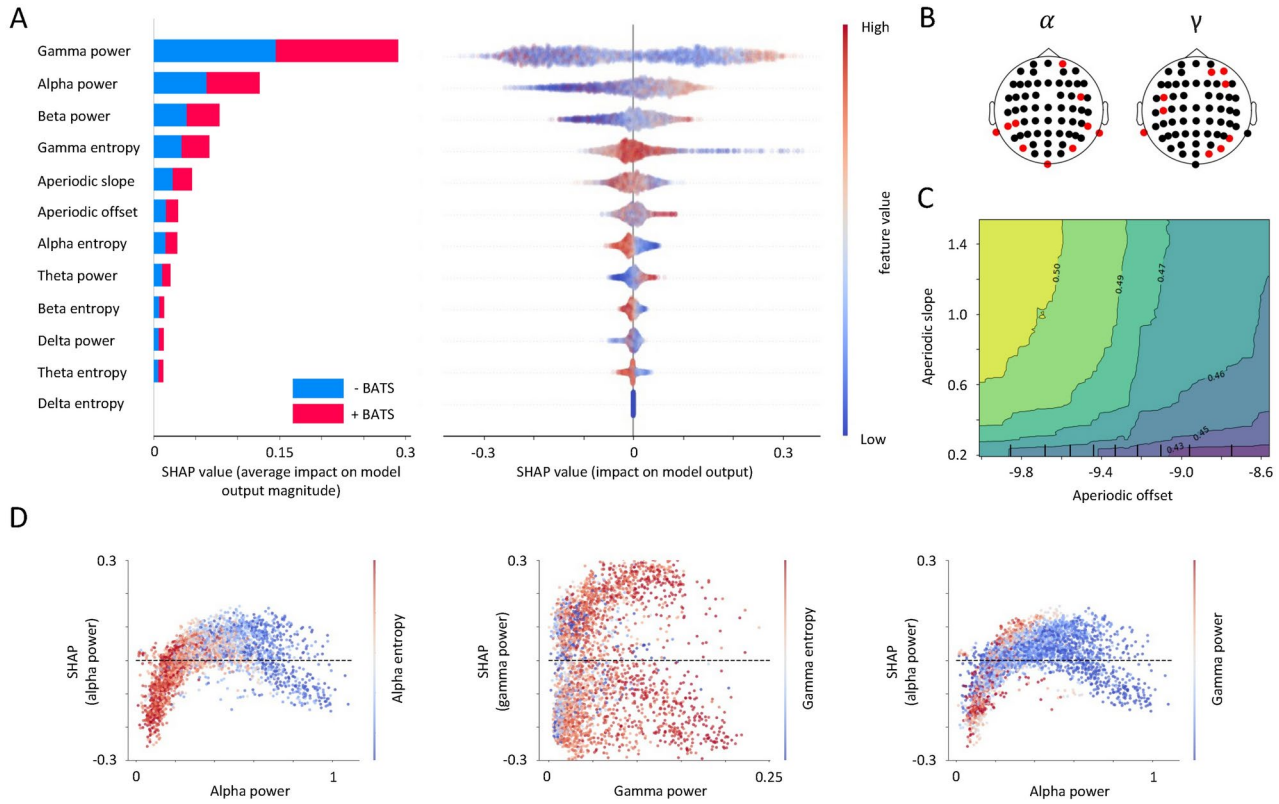

Fig. 3. Importance order and direction of the sensor space features on predicting +BATS. (**A**) On the left sub-panel, a list of sensor space features, arranged in decreasing order of importance in the classification procedure, is presented. The chart showcases the combined significance of features within each feature category for forecasting -BATS (absence of tinnitus acoustic suppression) and +BATS (presence of tinnitus acoustic suppression), indicated by blue and red colors correspondingly. The horizontal axis shows the averaged SHAP values associated with each feature category. Feature classes with higher average SHAP values have a greater impact on the prediction of targets. On the right sub-panel, the chart includes a collection of data points (i.e., single EEG epochs), which are placed horizontally across the x-axis, representing their respective SHAP values. Additionally, the color of each data point (epoch) reflects the feature values, with a gradient from red to blue representing high and low values. (**B**) Channels of significance in the alpha (left panel) and gamma (right panel) frequency ranges are highlighted in red. (**C**) Partial dependence plot displays the interaction between two feature sets (aperiodic offset and aperiodic slope) in predicting the class of individuals with +BATS. As the aperiodic offset decreases and the aperiodic slope increases, collectively indicating a reduction in non-oscillatory brain activity, there is a higher probability of predicting individuals with +BATS. (**D**) The x-axis of the scatter plots represents the values of alpha power (left and right sub-panels) and gamma power features (middle sub-panel). Each data point corresponds to an individual observation (i.e., a single EEG epoch) in the dataset. The y-axis represents the SHAP values associated with each feature for the same set of data points, and color gradients represent a third variable, namely, alpha entropy (left panel), gamma entropy (middle sub-panel), and gamma power (left and right subpanel). The baseline (y = 0, dotted line) represents the model's mean prediction of +BATS across all instances. Dots above the baseline indicate positive feature contribution, while dots below indicate negative feature contribution.

Taken together, the proposed and applied classification method seems to be very feasible to investigate trait-like neural features with regards to their predictive value on the ability to (acoustically) suppress tinnitus.

Neurophysiological relevance

Sensor space

In the first segment of our discussion, we focus on the model and features regarding the EEG sensor space. First, it's worth noting that higher gamma power values were more predictive of +BATS, with a distinct bias towards positive predictions but some negative extremes as well. In the absence of directly comparable experimental data, the discussion here is limited to links to general resting state data of tinnitus (trait-like) and to links to neural signatures during BATS (state-like). The latter comparison is especially precarious given the absence of state-like data and results in our study. Yet, looking at the pattern of positively-biased but bidirectional pattern of gamma features, our analysis aligns with the findings of Sedley et al. [31], where they argued that there was a positive correlation between tinnitus intensity and gamma band oscillations in the auditory cortex among a majority of patients (8 out of 14), suggesting an increased thalamocortical input and cortical gamma response

associated with higher tinnitus loudness. Conversely, all four patients exhibiting residual excitation (i.e., tinnitus loudness exceeding the baseline loudness before sound stimulation) demonstrated an inverse correlation between perceived tinnitus intensity and auditory cortex gamma oscillations. In a further study, it was shown that gamma oscillations are consistently more present during BATS [32], which was recently confirmed by another study [35], where an increase in alpha and gamma frequency bands during BATS was shown. Contrary to these positive gamma findings, two other studies could not find gamma and/or high frequency oscillation effects in BATS [34,65]. In our previous study, we observed decreased low gamma or high beta power post-stimulation (at 31 Hz), which was not linked to BATS [36]. The BATS experimental data regarding gamma thus seems to be inconclusive and, as introduced, considering general resting state data from tinnitus and basic literature about gamma or neural oscillations might be more productive. In comparison to healthy controls, increased gamma power in rest in individuals with chronic subjective tinnitus has been found in several studies [12–14,66]. In addition, some resting-state studies have shown a positive correlation between tinnitus loudness and gamma oscillations in auditory fields [67,68], which was also critically discussed in a position paper [69]. The pattern of increased high-frequency or gamma oscillations in tinnitus resting-state seems to be stable, with little contradicting evidence, and may be interpreted with the theorized higher neural synchrony in cortical auditory fields due to tinnitus [9,70]. Mapping these considerations back to our novel data, we certainly can assume that the gamma findings, including some bidirectional effects possibly related to individual differences, are reflected in our findings. Yet, it is not understood in detail how gamma oscillations may contribute to an active suppression of tinnitus. Gamma oscillations, typically in the range of 30–100 Hz, are closely associated with sensory processing, attention, and the integration of cortical information [71,72]. In the context of the auditory system, higher gamma power could reflect enhanced cortical excitability and increased neural synchrony within auditory pathways, which might be instrumental in the modulation or suppression of tinnitus. We thus theorize that increased trait-like gamma power and/or dynamics, as found in our study, might be aiding the cortical (auditory) system to suppress tinnitus. In addition, current considerations regarding the predictive brain might extend this reasoning by introducing that higher gamma activity in auditory cortical fields could be interpreted as the brain's attempt to enhance the precision of auditory predictions or to amplify the prediction error related to the phantom sound of tinnitus [32,73,74]. This increased activity could serve to better predict and, therefore, more effectively cancel out the internal representation of tinnitus, leading to its suppression.

Second, looking at the second most important identified feature, alpha power, the discussion of our finding of increased alpha power predictive of +BATS is more straightforward both given the clear direction of results and the results' fit to current theoretical models. Reduced (trait-like) alpha power in tinnitus has been consistently shown in resting state studies [12,75] and is theorized to be reflective of a disrupted (auditory) inhibitory system in tinnitus. Findings of reduced GABA, a major inhibitory neurotransmitter, concentration levels in cortical auditory fields may further corroborate the hypothesis of a defective inhibitory system in tinnitus [76,77]. A single study also showed that observed lower resting alpha power in tinnitus is correlated to higher gamma power linking the two major inhibitory and excitatory neural oscillations [66]. We could demonstrate a similar correlation in our analysis of +BATS prediction (see Fig. 3D). Furthermore, experimental data in BATS showing increases of alpha power during BATS confirms that BATS may temporarily restore normal cortical inhibition and thus suppress the perceived tinnitus sound [78]. Taken together, our results add to the importance of alpha regarding cortical inhibition and (acoustic) tinnitus suppression by establishing its importance as a trait-like feature in individuals with tinnitus, which has not been shown before.

Finally, aperiodic parameters complemented the results of the sensor feature set, demonstrating that +BATS is related to lower aperiodic offsets and steeper slopes, which suggest more periodic (i.e., oscillatory) activity over the entire power spectrum in individuals with +BATS (Fig. 3C). This observation fits considerations of thalamo-cortical dysrhythmia in tinnitus [79–81], expressed by a flatter overall M/EEG (resting state) spectrum and increases in high-frequency power (i.e., gamma).

Source space

Source localization of the identified most important features of the sensor model, gamma and alpha power, was motivated to constrain these findings to specific functionally-segregated brain regions. The discussion so far assumed that the effects to be mainly originating from cortical (bilateral) auditory fields, which is confirmed by the resulting sensor locations spanning lateral and posterior sensors (see Fig. 3D) and the bulk or previous literature. Regarding frequency-specific contributions in identified brain labels, global functional eminence of the alpha and gamma band in the context of tinnitus and sensory processes have to be elucidated: The prominence of alpha power in the right hemisphere and gamma in the left hemisphere suggests a division of labor between the hemispheres in general brain functioning [82]. Alpha oscillations generally reflect inhibitory processes and reduced cortical arousal [83], whereas gamma oscillations typically code sensory processing, attention, and the integration of cortical information [72]. Mapping these global and normal brain mechanisms to tinnitus and especially to trait-like features predicting tinnitus suppression is challenging in the absence of any relevant previous resting state data in tinnitus considered with lateralization of neural oscillations. Yet, our findings suggest that there is a correlation between the level of predictive gamma power in the left transverse temporal gyrus and predictive alpha power in the right transverse temporal gyrus (as shown in Fig. 4A, B), and the typical functioning preferences of the two hemispheres, particularly in the bilateral auditory cortex. This implies that normal brain functioning may be facilitating (acoustic) tinnitus suppression. Predictive trait-like gamma power in the left primary auditory cortex, namely transverse temporal or Heschl gyrus, may signify an adaptive neural process aimed at minimizing the sensory prediction errors that underlie the perception of tinnitus. In turn, such a minimization of prediction errors may contribute to successful tinnitus suppression.

In the insula, high alpha power is not predictive of +BATS, whereas the opposite pattern can be observed for alpha power in the rostral anterior cingulate cortex, posterior cingulate cortex, and superior frontal gyrus. In the

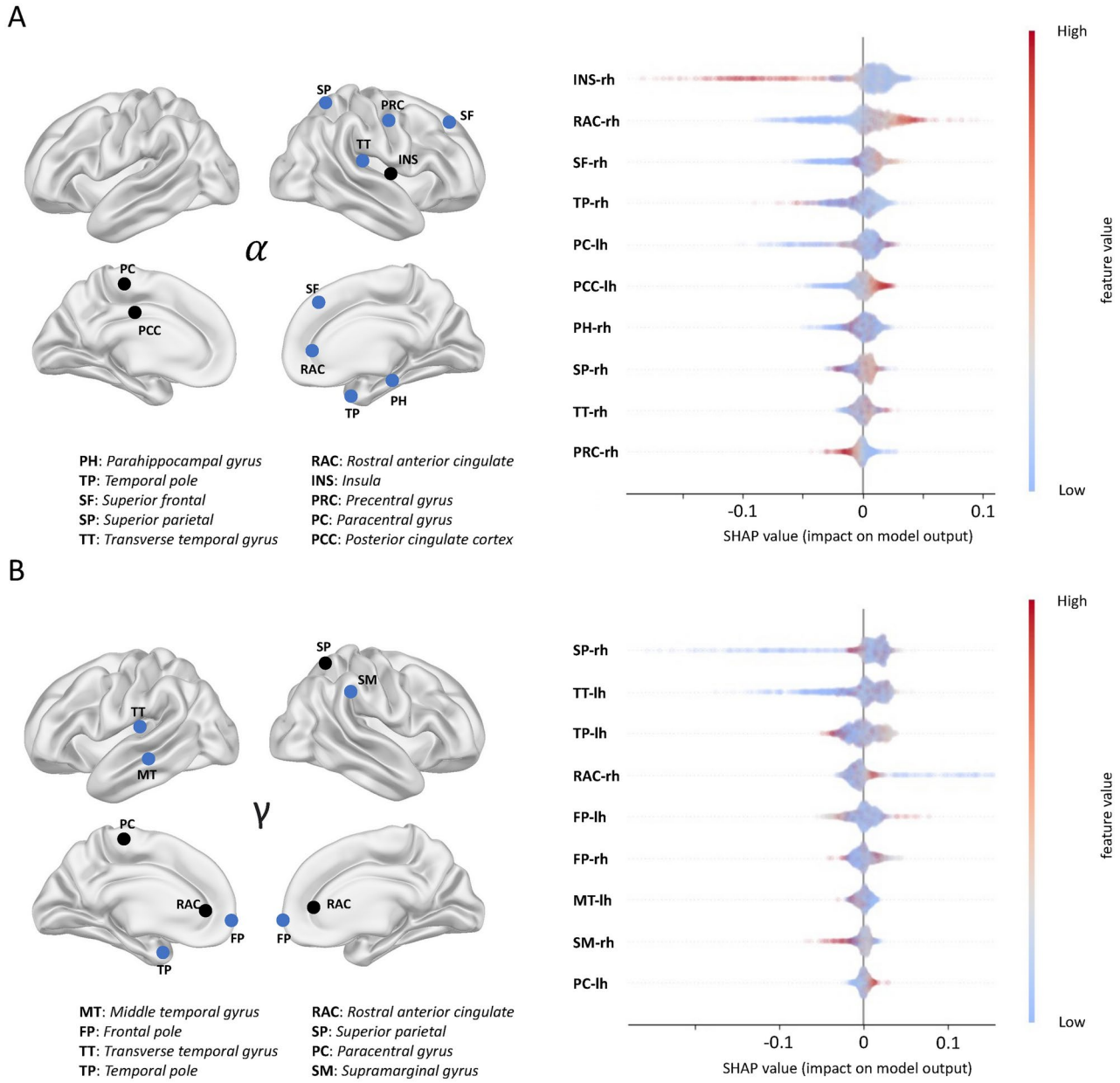

Fig. 4. The most contributing brain labels in prediction of +BATS. In both the alpha (**A**) and gamma (**B**) frequency range, brain labels that significantly contributed to predicting individuals with +BATS are denoted by circles. Brain labels shared with the validation dataset are highlighted in blue, while those not matching are colored in black. The importance and directionality of these brain labels in predicting +BATS are displayed in the right subpanels of (**A**, textbfB), respectively.

rostral anterior cingulate cortex, predictive trait-like alpha power could be linked to a functioning or maintained active tinnitus noise canceling system mediated through thalamocortical relays [84]. A correlative EEG resting state study has identified the anterior cingulate complex, including the rostral anterior cingulate cortex, to be involved in tinnitus perception [85]. Yet, the authors did not find any effects in the alpha frequency band. Moreover, also critical for our data, M/EEG source localization of deep, medial, and ventral structures like the subcallosal area, identified as the key node in the tinnitus noise-cancelling system [84,86], is challenging and possibly unreliable. Given structural vicinity and functional overlap of the anterior cingulate complex' subregions (i.e., rostral anterior cingulate cortex, pregenual anterior cingulate cortex, and subgenual anterior cingulate cortex), it was proposed by [87] to extend the functional locus of the key node of the noise-canceling system to the entirety of the ventromedial prefrontal cortex. Predictive trait-like alpha power in the posterior cingulate cortex could be both reflective of an intact DMN including its inhibitory properties and/or normal modes of memory processing, which could imply that tinnitus is not filled-in from the hippocampus as proposed in recent models [88,89]. In similar veins, predictive alpha in (superior) frontal regions could be indicative of functioning control (networks)

within the tinnitus brain, allowing for better attentional (or auditory gating) control and possibly suppression of the phantom sound perception [90]. Looking at gamma, its lack in superior parietal regions may be correlated to an absence of integration with other sensory systems (cross-modal compensation) and/or intact attentional or inhibitory control as in alpha and the posterior cingulate cortex [91,92]. Finally, the same could be true for a similar pattern in the rostral anterior cingulate cortex and, analogously to higher predictive alpha power in the same region, linked to an (intact) tinnitus noise canceling system.

Notably, identified regions also play a role in large and small-scale networks, such as, for example, the posterior cingulate cortex, a critical node in the default mode network. The involvement of the insula and the rostral anterior cingulate cortex highlights their significance in the salience network or ventral attention network, crucial for detecting and filtering salient external stimuli and internal events, thereby facilitating the transition between activated networks such as the default mode network and the central executive or frontoparietal network. The superior frontal gyrus and the frontal pole, implicated in executive function and attentional control, are key components of the frontoparietal network, underscoring their role in directing attention and managing cognitive resources, which could be particularly relevant in modulating attention towards or away from tinnitus sounds [93]. Additionally, the involvement of sensory integration and executive regions suggests a complex interplay between auditory processing and higher-order cognitive functions, emphasizing the multisensory and multidimensional nature of tinnitus perception within these overarching neural networks. Network aspects are further analyzed and discussed in the following section discussing our network model.

Connectivity

Looking at auditory connectivity, the specific intra-auditory alpha and gamma connections in +BATS individuals most probably reflect functioning inhibitory circuitry enabling the suppression of tinnitus (see Fig. 5C. The here observed intact connectivity contradicts findings of disrupted resting state alpha networks in individuals with tinnitus [94], implying that an intact intra-auditory network may support BATS. In the same study, authors found a resting state hyperconnection in the gamma frequency range which could be explained by differences in the analysis (i.e., resting state case-control design in the former study vs. within-group prediction in our study). In general, the resting state auditory network literature in tinnitus is not unequivocal, with conflicting results explained by the heterogeneity of the investigated tinnitus samples and/or applied methods [16].

On the large-scale network level, in the gamma frequency band, the most important connection of the connectivity RF model is found between AUN and SMN possibly related to increased sensory integration and/or attempts to minimize sensory prediction errors. Notably, both networks include the transverse temporal gyrus, which highlights their intrinsic connection and, thus, functional coupling. Further, a hyperconnection between AUN and the LBN could be representative of a trait-like intact noise canceling system [84], which may be further corroborated by a similar hyperconnection between AUN and the DGN including bilateral caudate, putamen, pallidum, and thalamus. However, given the large-scale character of investigated networks, more precise identification of medioventral key nodes of the proposed noise-canceling system (i.e., subgenual cingulate cortex and/or anterior cingulate cortex complex as well as the thalamus), can not be provided with our current data and analyses. Contrary to these hyperconnections, a hypoconnection between AUN and the (control) network FPN could be characteristic of a trait-like pattern of less attentional control and/or memory-related connectivity in +BATS individuals. This could imply that individuals with +BATS may not have developed aberrant network activity. The observed 3 hypoconnections between large-scale networks in the alpha frequency band, namely between VAN and DMN, AUN and DAN, and VAN and DGN, respectively, may echo the hypoconnection between AUN and FPN in the gamma frequency band. This would further corroborate the emerging pattern of hyperconnected auditory and/or potential noise-canceling networks in the absence of interactions between other large-scale networks and/or with the hyperconnected networks predicting +BATS.

Taken together, connectivity results of our 3rd model unfathomed a global pattern of intact intra-auditory connections in both frequency bands possibly implying functioning inhibitory and/or integrating auditory circuitry. Beyond that, large-scale networks are mostly hypoconnected, except auditory sensory as well as auditory limbic interactions, indicating normal functioning and/or an unimpaired noise-canceling system. The observed pattern of differential connectivity (hyper vs. hypoconnectivity) in auditory vs. attention/default mode networks may indicate a neural phenotype where 'normal' auditory processing, including tinnitus inhibition, remains relatively intact in the auditory network. This finding suggests that in this specific neural subtype of +BATS, more general networks may not yet be significantly involved or affected, potentially reflecting an earlier stage of tinnitus chronification or a distinct manifestation of individual trait-like neural profiles.

Behavioral differences

In our analysis, we observed higher MML and a trend towards higher tinnitus loudness levels in the -BATS group, suggesting a potential relationship between tinnitus perceptual intensity and the ability to achieve BATS. This observation is intriguing, especially given the absence of significant differences in tinnitus duration between groups, a marker often associated with tinnitus chronification. Constantly higher tinnitus loudness could be explained by a crossing of a non-linear threshold where the system's adaptive responses may become maladaptive. In consequence, certain inhibitory and/or neuroplastic mechanisms necessary for tinnitus suppression may become less effective [95,96]. This observation merits further investigation into the neural and perceptual dynamics underlying tinnitus and its modulation.

Limitations and future directions

The current study has some limitations that inform future studies in BATS, tinnitus research, and/or the methods applied.

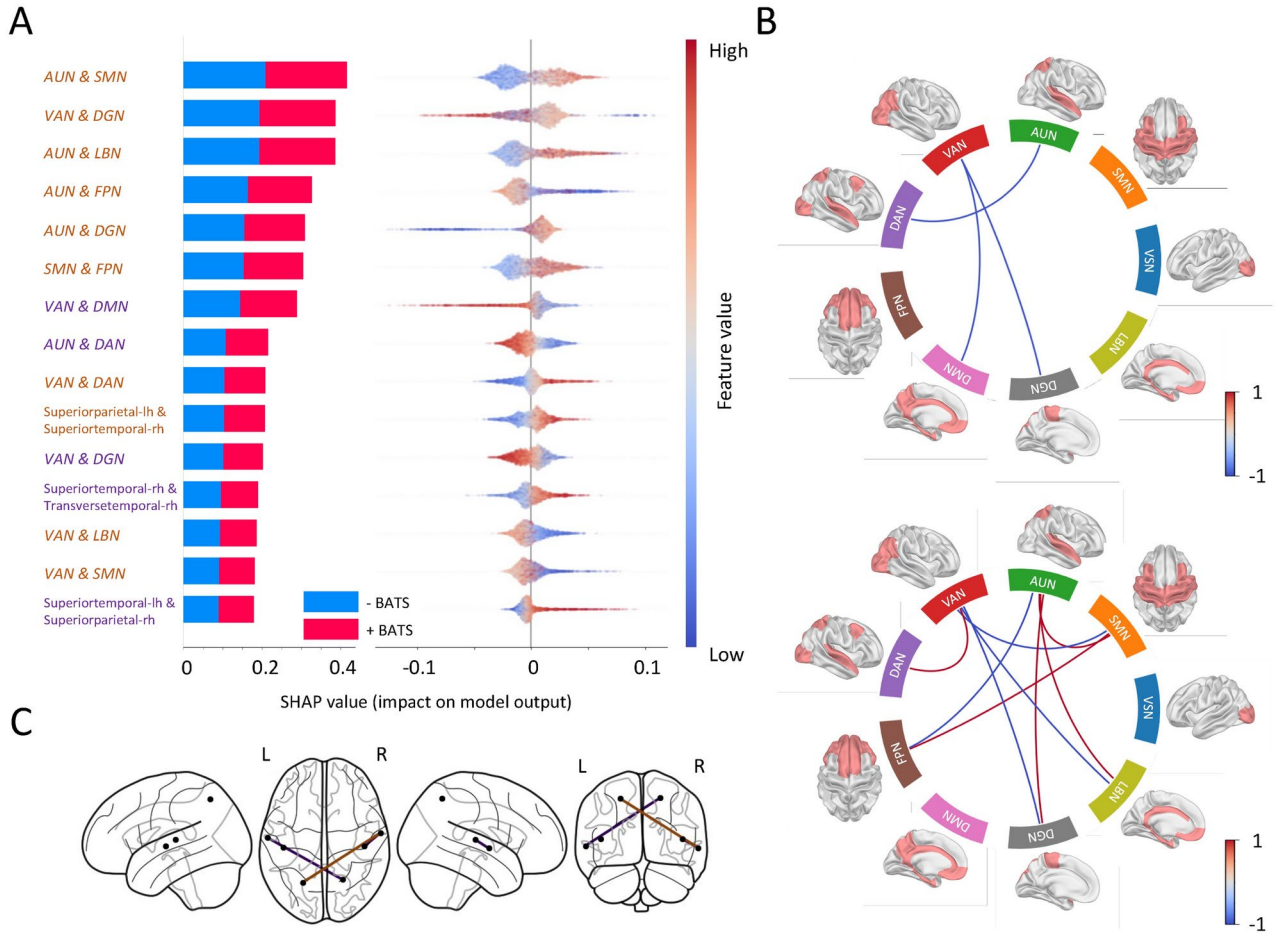

Fig. 5. Importance order and direction of the connectivity features on predicting +BATS. (**A**) The list of connections, sorted by importance in the classification process along with their directionality in predicting +BATS and -BATS, is presented. The y-axis tick labels, colored in purple and light brown, represent connections in the alpha and gamma frequency ranges, respectively. (**B**) The contrast between average connectivity across participants with +BATS and -BATS in alpha (upper panel) and gamma (bottom panel) within resting-state networks is depicted using circular graphs. The color gradient ranges from red to blue, indicating stronger connections in individuals with BATS ability to low values, indicating individuals with -BATS. (**C**) The most important connections within the AUN network in the classification process are visualized on a glass brain. Purple and light brown indicate connections in the alpha and gamma frequency ranges, respectively.

Classifier feature importance values and related ordered lists are delicate to interpret. Resulting values are not straightforward to interpret per se, especially if compared to modes of interpreting inferential frequentist or Bayesian statistics results. In a RF classifier, the Gini importance values, which quantify each feature's contribution to node purity and the overall quality of splits across the decision trees, do not necessarily sum to 1 but are scaled relative to each other. These values, reflective of a feature's frequency in splitting and its impact on reducing node impurity, vary with the data, the forest's size, and the algorithm's implementation, allowing for a meaningful comparison of feature importance within the model's context. SHAP values are used to explain the output of machine learning models by attributing the prediction to different features. They represent the contribution of each feature to the difference between the actual prediction and the average prediction. Each SHAP value corresponds to a feature and indicates how much that feature contributes to the prediction for a particular instance. Despite the complexities inherent in interpreting Gini importance and SHAP values within a RF classifier, our study's results remain reliable and interpretable, acknowledging the discussed limitations.

Gamma oscillations in resting-state EEG are often regarded as artifacts resulting from eye movements [97–100]. However, to prevent any influence on the results, activations associated with both vertical and horizontal eye movements were removed during preprocessing using ICA. Additionally, no behavioral differences-such as tinnitus distress, hearing, or overall health-were observed between the groups, further addressing this concern. Moreover, eye movements are unlikely to contribute to the differences observed between the two groups (positive and negative BATS).

Although there is no direct method to estimate the signal-to-noise ratio (SNR) of resting-state EEG signals, we aimed to enhance it during preprocessing. This was achieved by applying band-pass filters to minimize out-

of-band frequency interference, using ICA to remove artifacts, and manually discarding noisy epochs. While the power spectral density (PSD) does not explicitly quantify the SNR, it offers valuable insights into the quality of the recorded data (see supplementary Figure S4).

Even though our results are of high accuracy, stable over validation approaches, and meaningful in resulting features, larger sample sizes are needed to further consolidate and differentiate analyses and results. Yet, given our total sample size of 102 cases, the presented dataset is currently the largest in the context of EEG, BATS, and tinnitus.

Further, future studies could incorporate additional neurophysiological measures of higher spatial resolution, such as MRI, to complement the current feature sets and to ensure more precise source localization based on individual structural MRI in combination with scanned individual EEG electrode positions. Source localization may limit the precision of some of the presented data, which is discussed transparently throughout the paper.

To maximize the feature set included in machine learning modeling and, in consequence, derive insights in the spirit of explainable AI [38], further (neuro)physiological measures could be considered [101]. A maximized comprehensive feature set could lead to objective diagnosis and subtypization of tinnitus and/or the ability of tinnitus suppression [102,103].

Finally, by mapping the unique neural signatures associated with tinnitus in different individuals derived from our approach here, future studies could design targeted interventions that address the specific neural underpinnings of tinnitus in each individual. Such an approach would not only improve the precision of tinnitus treatments but also contribute to the broader field of personalized neurotherapy, optimizing interventions based on each individual's neural fingerprint.

Conclusion

The present work represents the first attempt to predict acoustic tinnitus suppression via spontaneous brain activity data. It aims to understand the potential suppression factors on the neural level through automatic classification and identification of distinctive features. Using a standard set of classifiers, we achieved high classification accuracy (98% for the sensor and source model and 86% for the connectivity model) with RF model and identified several, partly novel, trait-like neural features, which were further analyzed using the SHAP method. The resulting specific patterns of gamma and alpha oscillations in sensors and source-localized brain regions, especially with higher power in the alpha frequency band is predictive of +BATS, highlights the role of auditory cortical activity and its hemispheric distribution (i.e., right hemisphere dominance in alpha band and left hemisphere dominance in the gamma band) in managing phantom sound perception and suppression. Furthermore, we could demonstrate that intra-auditory and cross-network connectivity between large-scale (cortical) auditory and limbic networks were also predictive of an individual's ability to suppress tinnitus. Finally, by analyzing aperiodic features of the EEG power spectrum, it was shown that normal averaged spectral shapes are predictive of tinnitus suppression. Our approach advances the understanding of the neural basis of tinnitus suppression and tinnitus in general, highlighting distinct neural traits and dynamics between tinnitus subpopulations. This work not only paves the way for objective diagnosis and personalized treatment strategies but also underscores the potential for targeted, individualized interventions in tinnitus care.

Data availibility

The data can be obtained by other researchers upon reasonable request to the corresponding author (patrick.neff@uzh.ch). The analysis code is available at https://github.com/payamsash/Prime.

Received: 24 December 2024; Accepted: 20 March 2025
Published online: 31 March 2025

References

1. De Ridder, D. et al. Tinnitus and tinnitus disorder: Theoretical and operational definitions (an international multidisciplinary proposal). *Prog. Brain Res.* **260**, 1–25 (2021).
2. Baguley, D., McFerran, D. & Hall, D. Tinnitus. *Lancet* **382**, 1600–1607. https://doi.org/10.1016/S0140-6736(13)60142-7 (2013).
3. Jarach, C. M. et al. Global prevalence and incidence of tinnitus: A systematic review and meta-analysis. *JAMA Neurol.* **79**, 888–900 (2022).
4. Pinto, P. et al. Tinnitus and its association with psychiatric disorders: Systematic review. *J. Laryngol. Otol.* **128**, 660–664 (2014).
5. Langguth, B., Kleinjung, T., Schlee, W., Vanneste, S. & De Ridder, D. Tinnitus guidelines and their evidence base. *J. Clin. Med.* **12**, 3087 (2023).
6. Simoes, J. P. et al. Multidisciplinary tinnitus research: Challenges and future directions from the perspective of early stage researchers. *Front. Aging Neurosci.* **13**, 647285 (2021).
7. McFerran, D. J., Stockdale, D., Holme, R., Large, C. H. & Baguley, D. M. Why is there no cure for tinnitus?. *Front. Neurosci.* **13**, 802 (2019).
8. Langguth, B., Kreuzer, P. M., Kleinjung, T. & De Ridder, D. Tinnitus: Causes and clinical management. *Lancet Neurol.* **12**, 920–930. https://doi.org/10.1016/S1474-4422(13)70160-1 (2013).
9. Eggermont, J. J. & Tass, P. A. Maladaptive neural synchrony in tinnitus: Origin and restoration. *Front. Neurol.* **6**. https://doi.org/10.3389/fneur.2015.00029 (2015).
10. Elgoyhen, A. B., Langguth, B., De Ridder, D. & Vanneste, S. Tinnitus: Perspectives from human neuroimaging. *Nat. Rev. Neurosci.* **16**, 632–642. https://doi.org/10.1038/nrn4003 (2015).
11. Eggermont, J. J. & Roberts, L. E. The neuroscience of tinnitus: Understanding abnormal and normal auditory perception. *Front. Syst. Neurosci.* **6**. https://doi.org/10.3389/fnsys.2012.00053 (2012).
12. Weisz, N., Moratti, S., Meinzer, M., Dohrmann, K. & Elbert, T. Tinnitus perception and distress is related to abnormal spontaneous brain activity as measured by magnetoencephalography. *PLoS Med.* **2**, e153. https://doi.org/10.1371/journal.pmed.0020153 (2005).
13. Weisz, N. et al. The neural code of auditory phantom perception. *J. Neurosci.* **27**, 1479–1484. https://doi.org/10.1523/JNEUROSCI.3711-06.2007 (2007).

14. Ashton, H. et al. High frequency localised "hot spots" in temporal lobes of patients with intractable tinnitus: A quantitative electroencephalographic (QEEG) study. *Neurosci. Lett.* **426**, 23–28. https://doi.org/10.1016/j.neulet.2007.08.034 (2007).
15. Vanneste, S., Heyning, PVd. & Ridder, D. D. Contralateral parahippocampal gamma-band activity determines noise-like tinnitus laterality: A region of interest analysis. *Neuroscience* **199**, 481–490. https://doi.org/10.1016/j.neuroscience.2011.07.067 (2011).
16. Kok, T. E. et al. Resting-state networks in tinnitus. *Clin. Neuroradiol.* 1–20. https://doi.org/10.1007/s00062-022-01170-1 (2022).
17. Piarulli, A. et al. Tinnitus and distress: An electroencephalography classification study. *Brain Commun.* **5**, fcad018. https://doi.org/10.1093/braincomms/fcad018 (2023).
18. Jianbiao, M. et al. EEG signal classification of tinnitus based on SVM and sample entropy. *Comput. Methods Biomech. Biomed. Eng.* **26**, 580–594. https://doi.org/10.1080/10255842.2022.2075698 (2023).
19. Hong, E.-S., Kim, H.-S., Hong, S. K., Pantazis, D. & Min, B.-K. Deep learning-based electroencephalic diagnosis of tinnitus symptom. *Front. Hum. Neurosci.* **17**, 1126938 (2023).
20. Allgaier, J., Neff, P., Schlee, W., Schoisswohl, S. & Pryss, R. Deep learning end-to-end approach for the prediction of tinnitus based on EEG Data*. In *2021 43rd Annual International Conference of the IEEE Engineering in Medicine & Biology Society (EMBC)*. 816–819. https://doi.org/10.1109/embc46164.2021.9629964 (2021).
21. Neff, P. et al. 10 Hz amplitude modulated sounds induce short-term tinnitus suppression. *Front. Aging Neurosci.* **9**. https://doi.org/10.3389/fnagi.2017.00130 (2017).
22. Neff, P. et al. Comparison of amplitude modulated sounds and pure tones at the tinnitus frequency: Residual tinnitus suppression and stimulus evaluation. *Trends Hear* **23**, 2331216519833841. https://doi.org/10.1177/2331216519833841 (2019).
23. Schoisswohl, S. et al. Amplitude modulated noise for tinnitus suppression in tonal and noise-like tinnitus. *Audiol. Neurotol.* **24**, 309–321. https://doi.org/10.1159/000504593 (2019).
24. Tyler, R., Stocking, C., Secor, C. & Slattery, W. H. Amplitude modulated S-tones can be superior to noise for tinnitus reduction. *Am. J. Audiol.* **23**, 303. https://doi.org/10.1044/2014_AJA-14-0009 (2014).
25. Reavis, K. M. et al. Temporary suppression of tinnitus by modulated sounds. *J. Assoc. Res. Otolaryngol.* **13**, 561–571. https://doi.org/10.1007/s10162-012-0331-6 (2012).
26. Fournier, P. et al. A new method for assessing masking and residual inhibition of tinnitus. *Trends Hear* **22**. https://doi.org/10.1177/2331216518769996 (2018).
27. Neff, P. K. A. et al. Prolonged tinnitus suppression after short-term acoustic stimulation. *Prog. Brain Res.* https://doi.org/10.1016/bs.pbr.2021.02.004 (Elsevier, 2021).
28. Roberts, L. E. Residual inhibition. *Prog. Brain Res.* **166**, 487–495. https://doi.org/10.1016/S0079-6123(07)66047-6 (2007).
29. Roberts, L. E., Moffat, G., Baumann, M., Ward, L. M. & Bosnyak, D. J. Residual inhibition functions overlap tinnitus spectra and the region of auditory threshold shift. *J. Assoc. Res. Otolaryngol.* **9**, 417–435. https://doi.org/10.1007/s10162-008-0136-9 (2008).
30. Galazyuk, A. V., Longenecker, R. J., Voytenko, S. V., Kristaponyte, I. & Nelson, G. L. Residual inhibition: From the putative mechanisms to potential tinnitus treatment. *Hear Res.* **375**, 1–13. https://doi.org/10.1016/j.heares.2019.01.022 (2019).
31. Sedley, W. et al. Single-subject oscillatory gamma responses in tinnitus. *Brain* **135**, 3089–3100. https://doi.org/10.1093/brain/aws220 (2012).
32. Sedley, W. et al. Intracranial mapping of a cortical tinnitus system using residual inhibition. *Curr. Biol.* **25**, 1208–1214. https://doi.org/10.1016/j.cub.2015.02.075 (2015).
33. Kristeva-Feige, R., Feige, B., Kowalik, Z. & Ross, B. Neuromagnetic activity during residual inhibition in tinnitus. *J. Audiol. Med.* **4**, 135–142 (1995).
34. Kahlbrock, N. & Weisz, N. Transient reduction of tinnitus intensity is marked by concomitant reductions of delta band power. *BMC Biol.* **6**, 4. https://doi.org/10.1186/1741-7007-6-4 (2008).
35. King, R. O. C. et al. The effect of auditory residual inhibition on tinnitus and the electroencephalogram. *Ear Hear.* **42**, 130–141. https://doi.org/10.1097/AUD.0000000000000907 (2021).
36. Schoisswohl, S., Schecklmann, M., Langguth, B., Schlee, W. & Neff, P. Neurophysiological correlates of residual inhibition in tinnitus: Hints for trait-like EEG power spectra. *Clin. Neurophysiol.* **132**, 1694–1707 (2021).
37. Searchfield, G. D., Durai, M. & Linford, T. A state-of-the-art review: Personalization of tinnitus sound therapy. *Front. Psychol.* **8**, 1599 (2017).
38. Ali, S. et al. Explainable artificial intelligence (XAI): What we know and what is left to attain trustworthy artificial intelligence. *Inf. Fusion* **99**, 101805. https://doi.org/10.1016/j.inffus.2023.101805 (2023).
39. Doborjeh, M. et al. Prediction of tinnitus treatment outcomes based on EEG sensors and TFI score using deep learning. *Sensors* **23**, 902. https://doi.org/10.3390/s23020902 (2023).
40. Schiratti, J.-B., Le Douget, J.-E., Le Van Quyen, M., Essid, S. & Gramfort, A. An ensemble learning approach to detect epileptic seizures from long intracranial EEG recordings. In *2018 IEEE International Conference on Acoustics, Speech and Signal Processing (ICASSP)*. 856–860 (IEEE, 2018).
41. Craik, A., He, Y. & Contreras-Vidal, J. L. Deep learning for electroencephalogram (EEG) classification tasks: A review. *J. Neural Eng.* **16**, 031001 (2019).
42. Donoghue, T. et al. Parameterizing neural power spectra into periodic and aperiodic components. *Nat. Neurosci.* **23**, 1655–1665 (2020).
43. Çetin, F. H., Barış Usta, M., Aydın, S. & Güven, A. S. A case study on EEG analysis: Embedding entropy estimations indicate the decreased neuro-cortical complexity levels mediated by methylphenidate treatment in children with ADHD. *Clin. EEG Neurosci.* **53**, 406–417 (2022).
44. Aydın, S. Investigation of global brain dynamics depending on emotion regulation strategies indicated by graph theoretical brain network measures at system level. *Cognit. Neurodyn.* **17**, 331–344 (2023).
45. Desikan, R. S. et al. An automated labeling system for subdividing the human cerebral cortex on MRI scans into gyral based regions of interest. *Neuroimage* **31**, 968–980 (2006).
46. Buzsaki, G. *Rhythms of the Brain* (Oxford University Press, 2006).
47. Thomas Yeo, B. et al. The organization of the human cerebral cortex estimated by intrinsic functional connectivity. *J. Neurophysiol.* **106**, 1125–1165 (2011).
48. Li, J. et al. Exploring functional connectivity alterations in sudden sensorineural hearing loss: A multilevel analysis. *Brain Res.* **1824**, 148677 (2024).
49. Schober, P., Boer, C. & Schwarte, L. A. Correlation coefficients: Appropriate use and interpretation. *Anesth. Analgesia* **126**, 1763–1768 (2018).
50. Pedregosa, F. et al. Scikit-learn: Machine learning in python. *J. Mach. Learn. Res.* **12**, 2825–2830 (2011).
51. Breiman, L. Random forests. *Mach. Learn.* **45**, 5–32 (2001).
52. Friedman, J. H. Greedy function approximation: A gradient boosting machine. *Ann. Stat.* 1189–1232 (2001).
53. Duda, R. O. et al. *Pattern Classification and Scene Analysis* Vol. 3 (Wiley, 1973).
54. Lewis, D. D. Naive (Bayes) at Forty: The Independence Assumption in Information Retrieval. In *European Conference on Machine Learning*. 4–15 (Springer, 1998).
55. Hastie, T., Tibshirani, R., Friedman, J. H. & Friedman, J. H. *The Elements of Statistical Learning: Data Mining, Inference, and Prediction*. Vol. 2 (Springer, 2009).
56. Burges, C. J. A tutorial on support vector machines for pattern recognition. *Data Min. Knowl. Discov.* **2**, 121–167 (1998).
57. Rasmussen, C. E., Williams, C. K. et al. *Gaussian Processes for Machine Learning*. Vol. 1 (Springer, 2006).

58. Peterson, L. E. K-nearest neighbor. *Scholarpedia* **4**, 1883 (2009).
59. LeCun, Y., Bottou, L., Bengio, Y. & Haffner, P. Gradient-based learning applied to document recognition. *Proc. IEEE* **86**, 2278–2324 (1998).
60. Boser, B. E., Guyon, I. M. & Vapnik, V. N. A training algorithm for optimal margin classifiers. In *Proceedings of the Fifth Annual Workshop on Computational Learning Theory*. 144–152 (1992).
61. Lundberg, S. M. & Lee, S.-I. A unified approach to interpreting model predictions. In (Guyon, I. et al. eds.) *Advances in Neural Information Processing Systems* . Vol. 30. 4765–4774 (Curran Associates, Inc., 2017).
62. Jolliffe, I. T. *Principal Component Analysis for Special Types of Data* (Springer, 2002).
63. Weinberger, K. Q. & Saul, L. K. Distance metric learning for large margin nearest neighbor classification. *J. Mach. Learn. Res.* **10** (2009).
64. Gini, C. W. *Variability and Mutability, Contribution to the Study of Statistical Distributions and Relations* (Universita de Cagliari, Studi Economico-Giuridici della R, 1912).
65. Adjamian, P., Sereda, M., Zobay, O., Hall, D. A. & Palmer, A. R. Neuromagnetic indicators of tinnitus and tinnitus masking in patients with and without hearing loss. *J. Assoc. Res. Otolaryngol.* **13**, 715–731. https://doi.org/10.1007/s10162-012-0340-5 (2012).
66. Lorenz, I., Müller, N., Schlee, W., Hartmann, T. & Weisz, N. Loss of alpha power is related to increased gamma synchronization-A marker of reduced inhibition in tinnitus?. *Neurosci. Lett.* **453**, 225–228. https://doi.org/10.1016/j.neulet.2009.02.028 (2009).
67. Balkenhol, T., Wallhäusser-Franke, E. & Delb, W. Psychoacoustic tinnitus loudness and tinnitus-related distress show different associations with oscillatory brain activity. *PLoS One* **8**, e53180. https://doi.org/10.1371/journal.pone.0053180 (2013).
68. van der Loo, E. et al. Tinnitus intensity dependent gamma oscillations of the contralateral auditory cortex. *PLoS One* **4**, e7396. https://doi.org/10.1371/journal.pone.0007396 (2009).
69. Sedley, W. & Cunningham, M. O. Do cortical gamma oscillations promote or suppress perception? An under-asked question with an over-assumed answer. *Front. Hum. Neurosci.* **7**, 595. https://doi.org/10.3389/fnhum.2013.00595 (2013).
70. Uhlhaas, P. J. & Singer, W. Neural synchrony in brain disorders: Relevance for cognitive dysfunctions and pathophysiology. *Neuron* **52**, 155–168. https://doi.org/10.1016/j.neuron.2006.09.020 (2006).
71. Ray, S., Niebur, E., Hsiao, S. S., Sinai, A. & Crone, N. E. High-frequency gamma activity (80–150 Hz) is increased in human cortex during selective attention. *Clini. Neurophysiol.* **119**, 116–133. https://doi.org/10.1016/j.clinph.2007.09.136 (2008).
72. Schnitzler, A. & Gross, J. Normal and pathological oscillatory communication in the brain. *Nat. Rev. Neurosci.* **6**, 285–296. https://doi.org/10.1038/nrn1650 (2005).
73. Sedley, W., Friston, K. J., Gander, P. E., Kumar, S. & Griffiths, T. D. An integrative tinnitus model based on sensory precision. *Trends Neurosci.* **39**, 799–812. https://doi.org/10.1016/j.tins.2016.10.004 (2016).
74. Engel, A. K., Fries, P. & Singer, W. Dynamic predictions: Oscillations and synchrony in top-down processing. *Nat. Rev. Neurosci.* **2**, 704–716. https://doi.org/10.1038/35094565 (2001).
75. Schlee, W. et al. Reduced variability of auditory alpha activity in chronic tinnitus. *Neural Plast.* **1–9**, 2014. https://doi.org/10.1155/2014/436146 (2014).
76. Sedley, W. et al. Human auditory cortex neurochemistry reflects the presence and severity of tinnitus. *J. Neurosci.* **35**, 14822–14828. https://doi.org/10.1523/jneurosci.2695-15.2015 (2015).
77. Isler, B. et al. Lower glutamate and GABA levels in auditory cortex of tinnitus patients: A 2D-JPRESS MR spectroscopy study. *Sci. Rep.* **12**, 4068. https://doi.org/10.1038/s41598-022-07835-8 (2022).
78. Lange, J., Keil, J., Schnitzler, A., Dijk, Hv. & Weisz, N. The role of alpha oscillations for illusory perception. *Behav. Brain Res.* **271**, 294–301. https://doi.org/10.1016/j.bbr.2014.06.015 (2014).
79. Llinás, R. R., Ribary, U., Jeanmonod, D., Kronberg, E. & Mitra, P. P. Thalamocortical dysrhythmia: A neurological and neuropsychiatric syndrome characterized by magnetoencephalography. *PNAS USA* **96**, 15222–15227. https://doi.org/10.1073/pnas.96.26.15222 (1999).
80. Llinás, R., Urbano, F. J., Leznik, E., Ramírez, R. R. & van Marle, H. J. F. Rhythmic and dysrhythmic thalamocortical dynamics: GABA systems and the edge effect. *Trends Neurosci.* **28**, 325–333. https://doi.org/10.1016/j.tins.2005.04.006 (2005).
81. De Ridder, D., Vanneste, S., Langguth, B. & Llinas, R. Thalamocortical dysrhythmia: A theoretical update in tinnitus. *Front. Neurol.* **6**, https://doi.org/10.3389/fneur.2015.00124 (2015).
82. Zatorre, R. J. & Belin, P. Spectral and temporal processing in human auditory cortex. *Cereb. Cortex* **11**, 946–953. https://doi.org/10.1093/cercor/11.10.946 (2001).
83. Jensen, O. & Mazaheri, A. Shaping functional architecture by oscillatory alpha activity: Gating by inhibition. *Front. Hum. Neurosci.* **4**. https://doi.org/10.3389/fnhum.2010.00186 (2010).
84. Rauschecker, J. P., Leaver, A. M. & Mühlau, M. Tuning out the noise: Limbic-auditory interactions in tinnitus. *Neuron* **66**, 819–826. https://doi.org/10.1016/j.neuron.2010.04.032 (2010).
85. Song, J.-J., Vanneste, S. & Ridder, D. D. Dysfunctional noise cancelling of the rostral anterior cingulate cortex in tinnitus patients. *PLoS ONE* **10**, e0123538. https://doi.org/10.1371/journal.pone.0123538 (2015).
86. Meyer, M. et al. Differential tinnitus-related neuroplastic alterations of cortical thickness and surface area. *Hear. Res.* **342**, 1–12. https://doi.org/10.1016/j.heares.2016.08.016 (2016).
87. Rauschecker, J. P., May, E. S., Maudoux, A. & Ploner, M. Frontostriatal gating of tinnitus and chronic pain. *Trends Cognit. Sci.* **19**, 567–578. https://doi.org/10.1016/j.tics.2015.08.002 (2015).
88. Berger, J. I. et al. What is the role of the hippocampus and parahippocampal gyrus in the persistence of tinnitus?. *Hum. Brain Mapp.* **45**, e26627. https://doi.org/10.1002/hbm.26627 (2024).
89. Lee, S.-Y. et al. Is the posterior cingulate cortex an on-off switch for tinnitus?: A comparison between hearing loss subjects with and without tinnitus. *Hear. Res.* **411**, 108356. https://doi.org/10.1016/j.heares.2021.108356 (2021).
90. Knight, R. T., Scabini, D. & Woods, D. L. Prefrontal cortex gating of auditory transmission in humans. *Brain Res.* **504**, 338–342. https://doi.org/10.1016/0006-8993(89)91381-4 (1989).
91. Vanneste, S., Plazier, M., Loo, Evd, Heyning, PVd. & Ridder, D. D. The differences in brain activity between narrow band noise and pure tone tinnitus. *PLoS ONE* **5**, e13618 (2010).
92. Vanneste, S., Plazier, M., Loo, Evd, Heyning, PVd. & Ridder, D. D. The difference between uni- and bilateral auditory phantom percept. *Clin. Neurophysiol.* **122**, 578–587. https://doi.org/10.1016/j.clinph.2010.07.022 (2011).
93. Lee, S. J. et al. Triple network activation causes tinnitus in patients with sudden sensorineural hearing loss: A model-based volume-entropy analysis. *Front. Neurosci.* **16**, 1028776. https://doi.org/10.3389/fnins.2022.1028776 (2022).
94. Schlee, W., Hartmann, T., Langguth, B. & Weisz, N. Abnormal resting-state cortical coupling in chronic tinnitus. *BMC Neurosci.* **10**, 11. https://doi.org/10.1186/1471-2202-10-11 (2009).
95. Schaette, R. & Kempter, R. Computational models of neurophysiological correlates of tinnitus. *Front. Syst. Neurosci.* **6**, 34. https://doi.org/10.3389/fnsys.2012.00034 (2012).
96. Roberts, L. E. et al. Ringing ears: The neuroscience of tinnitus. *J. Neurosci.* **30**, 14972–14979. https://doi.org/10.1523/jneurosci.4028-10.2010 (2010).
97. Yuval-Greenberg, S., Tomer, O., Keren, A. S., Nelken, I. & Deouell, L. Y. Transient induced gamma-band response in EEG as a manifestation of miniature saccades. *Neuron* **58**, 429–441 (2008).
98. Hassler, U., Friese, U., Martens, U., Trujillo-Barreto, N. & Gruber, T. Repetition priming effects dissociate between miniature eye movements and induced gamma-band responses in the human electroencephalogram. *Eur. J. Neurosci.* **38**, 2425–2433 (2013).

99. Hassler, U., Barreto, N. T. & Gruber, T. Induced gamma band responses in human EEG after the control of miniature saccadic artifacts. *Neuroimage* **57**, 1411–1421 (2011).
100. Kober, S. E., Wood, G., Schuster, S. & Körner, C. Do miniature eye movements affect neurofeedback training performance? A combined EEG-eye tracking study. *Appl. Psychophysiol. Biofeedback* **49**, 313–327 (2024).
101. Tzounopoulos, T., Balaban, C., Zitelli, L. & Palmer, C. Towards a mechanistic-driven precision medicine approach for tinnitus. *J. Assoc. Res. Otolaryngol. JARO* **20**, 115–131. https://doi.org/10.1007/s10162-018-00709-9 (2019).
102. Jackson, R., Vijendren, A. & Phillips, J. Objective measures of tinnitus: A systematic review. *Otol. Neurotol.* **40**, 154–163. https://doi.org/10.1097/mao.0000000000002116 (2019).
103. Edvall, N. K. et al. Alterations in auditory brainstem response distinguish occasional and constant tinnitus. *J. Clin. Invest.* https://doi.org/10.1172/jci155094 (2022).

Acknowledgements
We are thankful to Susanne Staudinger, Anita Hafner, Bernhard Unsin, Kira Voigt, Jonathan Kisskalt, Anthony Ngu, Mariana Martins-Lopez, Deniza Avdi, Vithushika Raveenthiran, and Allegra Preisig for their invaluable help in study management and data acquisition. We thank all the participants for their efforts and patience in the partly tedious experimental procedures.

Funding
Payam S. Shabestari and Patrick Neff have been funded by SNF (Project Grant number 325130_208164) for this work.

Stefan Schoisswohl received funding from the dtec.bw - Digitalization and Technology Research Center of the Bundeswehr (MEXT project). dtec.bw is funded by the European Union NextGenerationEU.

Declarations

Competing interests
The authors declare no competing interests.

Additional information
Supplementary Information The online version contains supplementary material available at https://doi.org/10.1038/s41598-025-95351-w.

Correspondence and requests for materials should be addressed to P.N.

Reprints and permissions information is available at www.nature.com/reprints.

Publisher's note Springer Nature remains neutral with regard to jurisdictional claims in published maps and institutional affiliations.

Open Access This article is licensed under a Creative Commons Attribution 4.0 International License, which permits use, sharing, adaptation, distribution and reproduction in any medium or format, as long as you give appropriate credit to the original author(s) and the source, provide a link to the Creative Commons licence, and indicate if changes were made. The images or other third party material in this article are included in the article's Creative Commons licence, unless indicated otherwise in a credit line to the material. If material is not included in the article's Creative Commons licence and your intended use is not permitted by statutory regulation or exceeds the permitted use, you will need to obtain permission directly from the copyright holder. To view a copy of this licence, visit http://creativecommons.org/licenses/by/4.0/.

© The Author(s) 2025

Supplementary Material

Methods and supplemental information

EEG data and preprocessing

In the experiments performed at the University of Regensburg, resting state EEG was acquired for 10 minutes with alternating eyes open/closed blocks for 1 minute each on naive participants (i.e., no treatment or experimental procedures before the EEG recording). EEG was recorded with Brain Vision Recorder software (version 1.20, Brain Products GmbH, Gilching, Germany) together with a BrainAmp amplifier (Brain Products GmbH, Gilching, Germany) and an Easycap elastic electrode cap (Easycap GmbH, Herrsching, Germany) with 64 electrodes placed according to the 10-20 system[1,2]. EEG measurements were recorded at a sampling rate of 500 Hz and online referenced to FCz. Impedances were kept below 10 kOhm and balanced for all recordings.

In the experiments performed at the University of Zurich, the EEG resting state paradigm was identical to the Regensburg experiment and participants did also not undergo any treatment or experimental procedures before the EEG recording. The EEG system was from the same manufacturer but using a more current system with active electrodes. Brain Vision Recorder software (version 1.33, Brain Products GmbH, Gilching, Germany) in conjunction with a BrainAmp DC amplifier (Brain Products GmbH, Gilching, Germany) was used. Acticap Slim active electrode cap (Easycap GmbH, Herrsching, Germany) featuring 64 electrodes arranged in accordance with the international 10-20 system. Recordings were performed at a sampling rate of 1000 Hz, and online referencing was set relative to the FCz electrode. Impedances were kept below 10 kOhm and balanced for all recordings.

The EEG data was down-sampled to a sampling frequency of 250 Hz and before that, it underwent a lowpass filtering process with a cutoff frequency of 500 Hz to prevent signal aliasing in the down-sampling. Subsequently, the signals were filtered using a linear phase FIR filter with low and high cutoff frequencies of 1 and 80 Hz, respectively, in order to preserve the frequency content within different frequency bands. Additionally, a zero-phase FIR notch filter with a notch frequency at 50 Hz with stop and transition bands set to 0.25 and 1 Hz was applied to the data. This notch filter effectively eliminated any electrical interference or (line) noise around the 50 Hz frequency. The standard equidistant 10-20 system montage was used for electrode locations[1,2]. Using independent component analysis (ICA), the EEG data was separated into different components, and components related to eye blinks and eye movements were automatically identified and removed using the `MNE-ICALabel` python package[3]. The initial 3 seconds of each block (whether eyes open or closed) were excluded from the data to eliminate artifacts caused by the transition between eye opening or closing. The remainder of the EEG data blocks are then concatenated and segmented into 2-second epochs. We opted to use eyes closed epochs of the recordings to predict BATS to reduce vision artefacts and in accordance with previous works[4–6].

Feature extraction

In this study, we employed the `MNE` v.1.5.1 Python package[7] for preprocessing eeg recordings and computing power spectral density in both sensor and source spaces. The `FOOOF` v.1.1.0 Python package[8] was utilized to compute the aperiodic components (offset and slope) of the power spectral density. For assessing spectral connectivity within brain labels, we utilized the `MNE-Connectivity` v.0.5 package[9]. In addition, `scikit-learn` v.1.3.1[10] was used for the classification tasks, and the `SHAP` v.0.43.0 package[11] was employed to evaluate the direction and importance of features in the classification task.

Spectral band power

The average power of a signal was calculated within five specific frequency ranges: delta (0.5–4.5 Hz), theta (4.5–8.5 Hz), alpha (8.5–13.5 Hz), beta (15–30 Hz), and gamma (30–80 Hz)[12]. This computation was performed for each epoch using *multitaper* spectral estimation method[7,13], in which the signal is convolved with a set of optimal bandpass filters known as DPSS filters and the the final power spectral density is obtained by averaging resulting power spectra over all the filters. The bandwidth of the chosen tapers is set to 8 divided by the duration of each epoch, which is equivalent to 4 Hz. For a selected frequency range, the frequencies within ± half of the bandwidth (i.e., bandwidth / 2) are smoothed together to obtain the power estimate[14]. As a result, the number of band power features is equal to 310 (5 * 62), which represents the number of frequency ranges multiplied by the number of channels.

Spectral entropy

We computed Shannon entropy to quantify the degree of disorder or uncertainty in the distribution of power across different frequency components in a signal's spectrum. It provides a measure of the diversity or randomness of frequency content within a signal's spectral profile. Spectral Shannon entropy is calculated as follows for each individual epoch within each frequency range: first we computed the power spectral density (PSD) of the epochs within the specific frequency range as described in . Then we normalized the PSD values to obtain a probability distribution. This involves dividing the PSD values by the sum

of PSD values within that frequency range for that specific channel, ensuring that the probabilities sum up to 1. Finally we Calculated the Shannon entropy for that channel and frequency range using the following formula:

$$H = -\sum_{i=1}^{N} P(f_i) \cdot \log_2[P(f_i)] \tag{1}$$

where H represents the Spectral Shannon entropy. N is the total number of frequency components or bins in the spectrum and $P(f_i)$ is the probability (or normalized power) associated with the i th frequency component in the spectrum.

Aperiodic spectral power

In order to calculate the aperiodic broadband and exponent parameters for each epoch, we used the `FOOOF` Python module[8]. This package allows for the parameterization of the estimated power spectrum density (PSD). Specifically, it models the non-oscillatory portion of the PSD, which exhibits a 1/f-like behavior, using an exponential function as noted in the following equation:

$$AP(f) = 10^b \cdot \frac{1}{(k + f^x)} \tag{2}$$

where b is the broadband offset, k indicates the 'knee' parameter for controlling the bend in the spectrum and x denotes the aperiodic slope. By fitting this model, the aperiodic broadband offset and exponent parameters can be obtained for further analysis and interpretation. 124 (62 * 2) features representative of aperiodic activity used for classification purposes.

Source space power spectral density

To calculate an approximate forward operator for our EEG recordings, we utilized the boundary element model, source model, and co-registration information of a standard template MRI subject from the `MNE` python package[7]. In our EEG recordings, since there was no specific period of the data available for estimating the noise covariance, we used an ad hoc covariance matrix for noise modeling within our EEG sensors. This ad hoc covariance matrix is equivalent to what we would obtain for Gaussian noise on the sensors, assuming an infinite number of samples. This approach is a practical way to account for sensor noise in the absence of direct noise estimation from the data. Utilizing the noise covariance and forward solution, we employed the linear minimum-norm inverse method known as "*dSPM*" to determine the inverse solution[7]. This allowed us to obtain source time courses and source power spectra. For each brain label, we extracted a single time course by averaging across vertices at each time point within each label[7]. The brain labels and cortical parcellation were derived from the Desikan-Killiany Atlas[15]. The number of features that represent the power of brain labels is 340 which is equal to number of frequency ranges * number of brain labels.

Connectivity measure

To estimate spectral densities for coherence calculation, we employed a continuous wavelet transform utilizing Morlet wavelets with 7 cycles and a zero mean. The temporal window decreases proportionally with frequency, scaling by the number of cycles. The formula employed to subsequently compute coherence between two epochs at a specific frequency component is as follows:

$$C(f) = \frac{|S_{xy}(f)|^2}{S_{xx}(f) \cdot S_{yy}(f)} \tag{3}$$

where Cross-Power Spectral Density $S_{xy}(f)$ indicate the degree to which the two epochs are correlated at a specific frequency. It accounts for both phase and magnitude information. A high magnitude of $S_{xy}(f)$ suggests strong correlation. Power Spectral Densities $S_{xx}(f)$ and $S_{yy}(f)$ measure the power or energy contained in each epoch at the same frequency and the coherence value $C(f)$ indicates the relationship or coherence between the two epochs at frequency f ranging between 0 and 1. We computed the spectral connectivity between all pairs of brain regions delineated by the 'Desikan-Killiany' cortical atlas, considering the two distinct frequency ranges: alpha and gamma.

Feature importance and directionality

We used Gini index[16] as an indicator of feature importance in our classification process using RF with 100 trees (estimators) in the forest. In a classification problem, the Gini impurity for a node is calculated as follows:

$$Gini(node) = 1 - \sum_{i=1}^{C} (p_i)^2 \tag{4}$$

where C is the number of classes and p_i is the probability of an element in the node belonging to class i. Feature importance is determined by aggregating the decrease in Gini impurity achieved by each feature when it is used to split nodes across all the trees in the forest. Features that consistently lead to a significant reduction in Gini impurity are considered more important, as they contribute more to the classification accuracy.

To assess the directionality of the features on the model prediction, we used `SHAP` Python pacckage[11]. `SHAP` calculates Shapley values from cooperative game theory. Shapley values allocate a contribution score to each feature based on its collaboration with other features in predicting a specific outcome. These scores represent the impact of each feature on a model's prediction. Following is the equation to compute Shapley values for each individual feature:

$$\phi_i(f) = \frac{1}{N} \sum_{S \subseteq N \setminus \{i\}} \binom{N-1}{|S|}^{-1} (val(S \cup \{i\}) - val(S)) \tag{5}$$

in which, represents $\phi_i(f)$ the SHAP value for feature i. N is the total number of features. S is a subset of features that excludes feature i. val(S) represents the model's output (e.g., prediction) for the subset of features S and $\binom{N-1}{|S|}$ denotes the number of ways to choose a subset of features S from the remaining $N-1$ features. `SHAP` generates interpretable explanations for individual predictions (i. e. +BATS and -BATS). For a given prediction, it quantifies how much each feature contributed to pushing the model's prediction away from a baseline or reference prediction. This attribution helps to understand not only which features are important but also in which direction they influence the prediction. Positive SHAP values indicate that a feature contributes to increasing the prediction, while negative values suggest that a feature contributes to decreasing the prediction. This directionality allows to grasp whether a feature has a positive or negative impact on the classifier outcome.

Tables

Table S1. Sample description. All dB values are in dB SPL (sound pressure level). M = mean; SD = standard deviation; Md = median; BATS = brief acoustic tinnitus suppression. BATS levels refer to the perceived tinnitus loudness after sound stimulus offset.

	Main dataset					**Validation dataset**				
N (female)	73 (38)					29 (4)				
Tinnitus side (left/ right/ bilateral)	(7/ 13/ 53)									
	M	**SD**	**Md**	**Min**	**Max**	**M**	**SD**	**Md**	**Min**	**Max**
Age (years)	52.60	10.84	55.00	23.00	69.00	41.19	13.62	35.00	22.00	66.00
Tinnitus duration (months)	118.81	70.84	110.00	18.00	280.00	112.32	107.00	60.00	6.00	380.00
Hearing loss (both ears, dB)	21.70	12.41	21.69	-7.22	53.06	6.996	6.41	8.42	-1.91	18.44
MML (dB)	62.91	16.45	60.65	30.10	90.00	51.81	20.13	55.50	1.00	85.00
THI total score (0-100)	37.26	24.08	34.00	4.00	98.00	38.54	17.59	36.00	12.00	84.00
GUF total score	11.30	6.95	10.00	0.00	34.00	6.65	4.85	6.50	0.00	16.00
Tinnitus loudness (dB)	54.96	17.52	52.00	27.00	90.00					
BATS (%) / BATS (-5 - +2)*	86.35	18.82	93.21	7.59	107.14	-0.92	2.23	0.00	-5.00	1.00

Table S2. Descriptive statistics of sample split in the main dataset. No differences in key variables between the groups except for MML (higher in -BATS). All dB values are in dB SPL (sound pressure level). SD = Standard Deviation.

Variable	Mean (SD)		Difference statistics	
	+BATS	-BATS	Statistics	p-value
Age (years)	54.40 (9.40)	51.24 (11.87)	t=1.255	0.214
Sex (female)	35 (16)	38 (22)	chi=0.650	0.420
THI total score (0-100)	34.86 (25.73)	39.47 (22.58)	t=-0.816	0.417
Hearing loss (both ears, dB)	25.38 (9.51)	23.06 (11.96)	t=0.914	0.364
tinnitus duration (months)	114.17 (73.32)	123.08 (69.17)	t=-0.534	0.595
tinnitus frequency	6098.14 (2684.83)	6122.39 (3229.57)	t=-0.035	0.972
MML (dB)	60.03 (16.87)	67.66 (14.84)	t=-2.054	**0.044**
tinnitus loudness (dB)	54.71 (22.46)	63.29 (22.03)	t=-1.646	0.104
Hyperacusis score (0-45)	10.34 (7.49)	12.18 (6.38)	t=-1.133	0.261

Table S3. Overview of brain regions extracted from Desikan-Killiany atlas and assigned to 9 sub-networks. For each brain parcel both left and right hemispheres are assigned to the correponding sub-network.

Network name	**Included brain labels**
VSN (visual network)	cuneus - lingual - lateraloccipital -pericalcarine
SMN (somatomotor network)	caudalmiddlefrontal - postcentral - precentral - paracentral - transversetemporal
AUN (auditory network)	superiorparietal - superiortemporal - transversetemporal
VAN (ventral attention network)	fusiform - inferiorparietal - lingual - lateraloccipital
DAN (dorsal attention network)	caudalmiddlefrontal - lateraloccipital - paracentral - superiorparietal - superiortemporal
FPN (frontoparietal network)	lateralorbitofrontal - parsopercularis - parsorbitalis - parstriangularis - rostralmiddlefrontal - superiorfrontal - superiortemporal
DMN (default mode network)	caudalanteriorcingulate - entorhinal - frontalpole - isthmuscingulate - medialorbitofrontal - parahippocampal - posteriorcingulate - precuneus - rostralanteriorcingulate
DGN (deep grey matter network)	caudalmiddlefrontal - paracentral - postcentral - precentral - superiorparietal - superiortemporal
LBN (limbic network)	caudalanteriorcingulate - entorhinal - frontalpole - isthmuscingulate - medialorbitofrontal - parahippocampal - posteriorcingulate

Table S4. Random Forest classifier performance. Metrics evaluating performance, such as accuracy, precision, recall, and F1-score, are provided for each classification task, encompassing both the primary dataset and the validation dataset.

	Main dataset				Validation dataset			
	accuracy	*precision*	*recall*	*f1-score*	*accuracy*	*precision*	*recall*	*f1-score*
Sensor space features	98%	98%	98%	98%	96%	96%	96%	96%
Source space features	98%	98%	98%	98%	99%	99%	99%	99%
Connectivity features	86%	86%	86%	86%	82%	82%	81%	80%

Figures

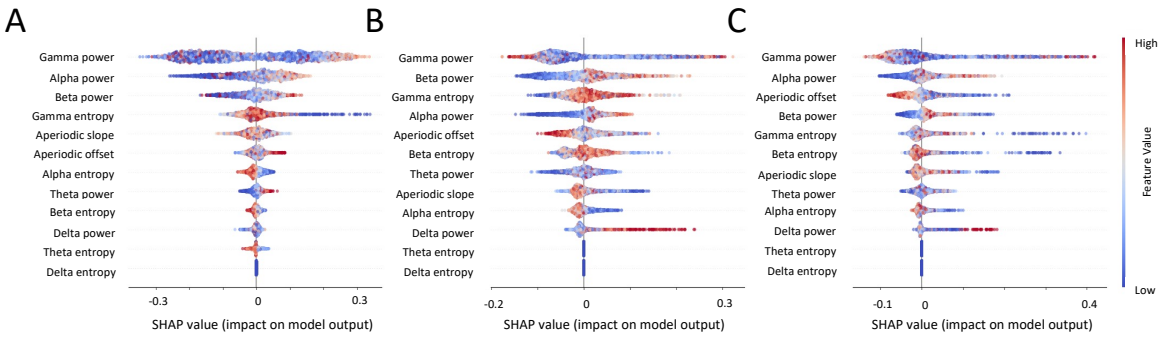

Figure S1. Importance order and directionality of sensor space features are shown for three different loudness threshold value, namely 90 (A), 70 (B) and 50 (C). The dots at each plot indicate SHAP values measuring how much each feature category contributes to predicting class of individuals with +BATS. Furthermore, the color of each data point (epoch) represents the feature values, following a gradient from red to blue, where red indicates high values, and blue signifies low values.

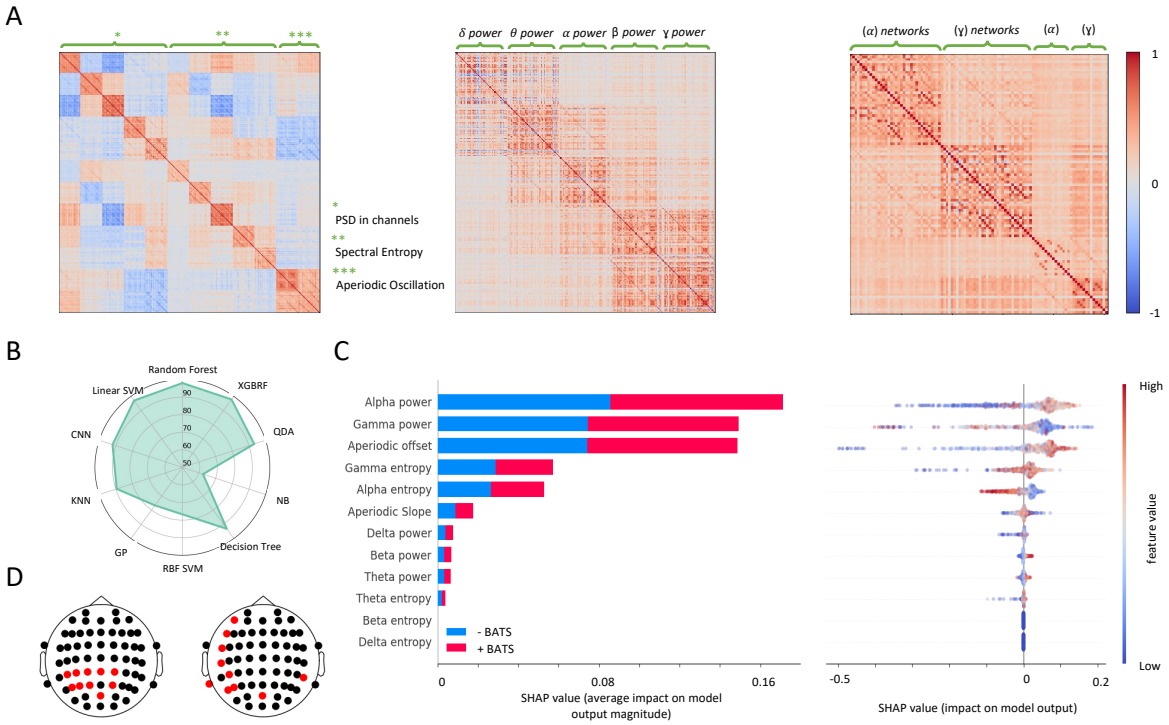

Figure S2. Analysis of validation dataset. A. Visual representation of the correlation matrix of the validation dataset, showing the relationships between various pairs of features including computed features in sensor space (left panel), source space (middle panel) and connectivity features (right panel). To reduce multicollinearity among features, values greater than 0.9 are combined. **B**. Accuracy values of ten distinct classifiers applied on the EEG epochs of validation dataset. **C**. Sensor space features are organized by decreasing importance for predicting two classes: +BATS and -BATS. In the left panel, the horizontal axis displays averaged SHAP values for each feature category, with higher values indicating greater influence on target prediction. Right panel consists of data points (epochs), representing feature categories, placed along the x-axis based on their SHAP values. Data point colors range from red to blue, reflecting feature values from high to low. **D**. Most contributing channels in classifying individuals with +BATS and -BATS are colored in red in both alpha (right panel) and gamma (left panel) frequency ranges.

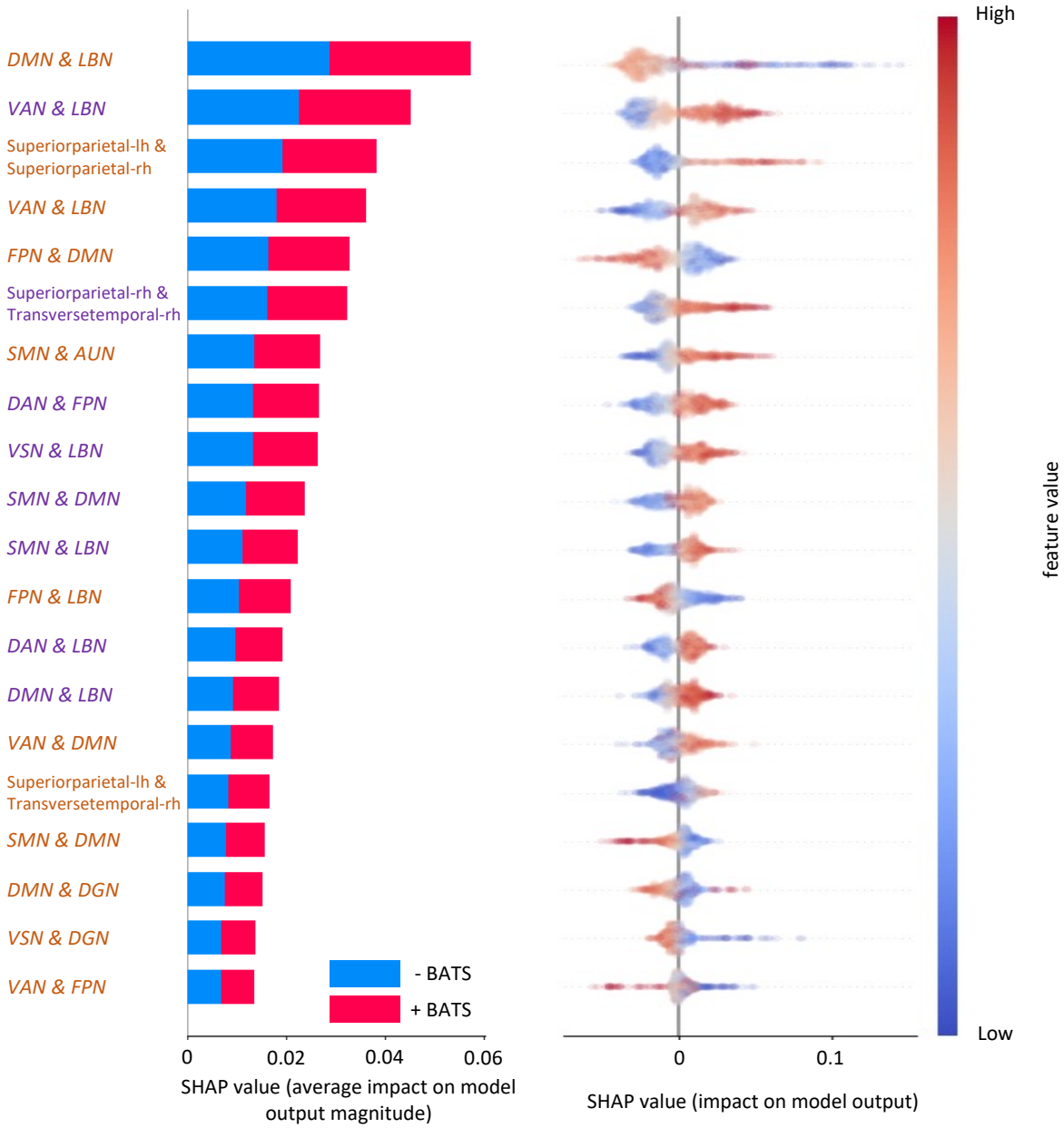

Figure S3. The list of most contributing connections in the validation dataset, sorted by their importance in the classification process. Each connection's directionality is also shown. The y-axis tick labels, colored in purple and light brown, correspond to connections in the alpha and gamma frequency ranges, respectively.

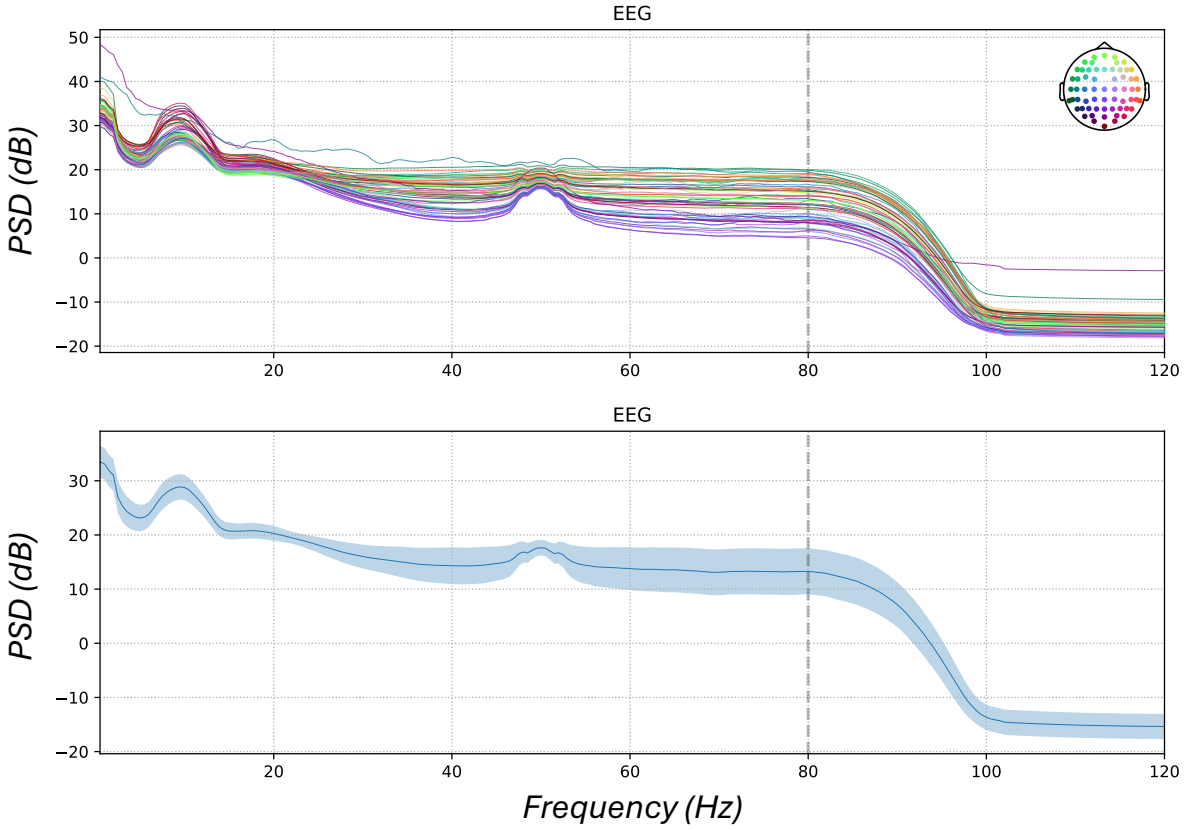

Figure S4. The power spectral density (PSD) of the main dataset, averaged across all subjects, is displayed for the 0–120 Hz frequency range. The top plot presents the PSD for individual channels, while the bottom plot features a blue ribbon illustrating the standard deviation of PSD across both subjects and channels. A dashed vertical line marks the high-cut frequency of the band-pass filter at 80 Hz.

References

1. Jurcak, V., Tsuzuki, D. & Dan, I. 10/20, 10/10, and 10/5 systems revisited: their validity as relative head-surface-based positioning systems. *Neuroimage* **34**, 1600–1611 (2007).
2. Oostenveld, R. & Praamstra, P. The five percent electrode system for high-resolution eeg and erp measurements. *Clin. neurophysiology* **112**, 713–719 (2001).
3. Li, A., Feitelberg, J., Saini, A. P., Höchenberger, R. & Scheltienne, M. Mne-icalabel: Automatically annotating ica components with iclabel in python. *J. Open Source Softw.* **7**, 4484 (2022).
4. Li, Z. *et al.* Objective recognition of tinnitus location using electroencephalography connectivity features. *Front. Neurosci.* **15**, 784721 (2022).
5. Li, J. *et al.* Exploring functional connectivity alterations in sudden sensorineural hearing loss: A multilevel analysis. *Brain Res.* **1824**, 148677 (2024).
6. Piarulli, A. *et al.* Tinnitus and distress: an electroencephalography classification study. *Brain communications* **5**, fcad018 (2023).
7. Gramfort, A. *et al.* Meg and eeg data analysis with mne-python. *Front. neuroscience* 267 (2013).
8. Donoghue, T. *et al.* Parameterizing neural power spectra into periodic and aperiodic components. *Nat. neuroscience* **23**, 1655–1665 (2020).
9. Li, A. *et al.* mne-connectivity (2022).
10. Pedregosa, F. *et al.* Scikit-learn: Machine learning in python. *J. machine Learn. research* **12**, 2825–2830 (2011).
11. Lundberg, S. M. & Lee, S.-I. A unified approach to interpreting model predictions. In Guyon, I. *et al.* (eds.) *Advances in Neural Information Processing Systems 30*, 4765–4774 (Curran Associates, Inc., 2017).
12. Buzsaki, G. *Rhythms of the Brain* (Oxford university press, 2006).
13. Percival, D. B. & Walden, A. T. *Spectral analysis for physical applications* (cambridge university press, 1993).
14. Slepian, D. Prolate spheroidal wave functions, fourier analysis, and uncertainty—v: The discrete case. *Bell Syst. Tech. J.* **57**, 1371–1430 (1978).
15. Desikan, R. S. *et al.* An automated labeling system for subdividing the human cerebral cortex on mri scans into gyral based regions of interest. *Neuroimage* **31**, 968–980 (2006).
16. Gini, C. W. Variability and mutability, contribution to the study of statistical distributions and relations. *Studi Econ. della R. Univ. de Cagliari* (1912).

STIFTUNG TINNITUS & HÖREN CHARITÉ

Research. Educate. Alleviate.

Application Form for the Research Award Tinnitus & Hearing 2024

We kindly ask you to fill in as well as sign this form and to attach a scan of your application to your e-mail or include a copy of your application with your letter.

1. Confirmation of exclusive submission

[X] I hereby confirm that the scientific work submitted for the Research Prize Tinnitus & Hearing 2024 has not been submitted for any other prize and that this work will not be submitted for any other prize until the decision on the award of the prize has been made.

2. Confirmation of authorship

The scientific work submitted by me for the Research Prize Tinnitus & Hearing 2024 involved several authors:

[X] Yes [ ] No

The following person is applying for the award (surname, first name)

Neff, Patrick

I hereby confirm that all authors and co-authors of the submitted work agree to the application for the Research Prize Tinnitus & Hearing 2024.

[X] Yes

Zürich	30.9.2025	Neff, Patrick	
Place	Date	Name, First Name	Signature